

A BOUNDED ARTIFICIAL VISCOSITY LARGE EDDY SIMULATION MODEL

JEFF BORGGAARD ^{*}, TRAIAN ILIESCU [†], AND JOHN PAUL ROOP [‡]

Abstract. In this paper, we present a rigorous numerical analysis for a bounded artificial viscosity model ($\tau = \mu\delta^\sigma a(\delta\|\nabla^s \mathbf{u}\|_F)\nabla^s \mathbf{u}$) for the numerical simulation of turbulent flows. In practice, the commonly used Smagorinsky model ($\tau = (c_s\delta)^2\|\nabla^s \mathbf{u}\|_F \nabla^s \mathbf{u}$) is overly dissipative, and yields unphysical results. To date, several methods for “clipping” the Smagorinsky viscosity have proven useful in improving the physical characteristics of the simulated flow. However, such heuristic strategies rely strongly upon *a priori* knowledge of the flow regime. The bounded artificial viscosity model relies on a highly nonlinear, but monotone and smooth, semilinear elliptic form for the artificial viscosity. For this model, we have introduced a variational computational strategy, provided finite element error convergence estimates, and included several computational examples indicating its improvement over the overly diffusive Smagorinsky model.

Key words. Large eddy simulation, turbulence, artificial viscosity, Smagorinsky model

AMS subject classifications. 15A15, 15A09, 15A23

1. Introduction. Turbulence is central to many important applications. Direct numerical simulation is not feasible for the foreseeable future in many of these applications. Indeed, Kolmogorov’s 1941 theory (K-41) of homogeneous, isotropic turbulence predicts that small scales exist down to $O(Re^{-3/4})$, where $Re > 0$ is the Reynolds number. Thus, in order to capture all scales on a mesh, we need a mesh-size $h \sim Re^{-3/4}$, and consequently (in 3D) $N \sim Re^{9/4}$ mesh points.

Large eddy simulation (LES) is one of the most successful approaches in the numerical simulation of turbulent flows. LES seeks to calculate the large, energetic structures (the large eddies) in a turbulent flow. The large structures are defined by convolving the flow variables with a rapidly decaying spatial filter g_δ . To derive equations for $\bar{\mathbf{u}}$, the large eddy flow structure, we convolve the NSE with $g_\delta(\mathbf{x})$. The resulting system is not closed, since it involves both \mathbf{u} and $\bar{\mathbf{u}}$. The tensor $\boldsymbol{\tau}(\mathbf{u}, \mathbf{u}) = \overline{\mathbf{u}\mathbf{u}^T} - \bar{\mathbf{u}}\bar{\mathbf{u}}^T$ is often called the subgrid-scale stress (SGS) tensor. Thus, the closure problem in LES is to model the SGS tensor $\boldsymbol{\tau}(\mathbf{u}, \mathbf{u})$.

The simplest and most commonly used approach to the closure problem is the Eddy Viscosity (EV) model. EV models are motivated by the idea that the global effect of the SGS stress tensor $\boldsymbol{\tau}(\mathbf{u}, \mathbf{u})$, in the mean, is to transfer energy from resolved to unresolved scales through inertial interactions [19, 42, 47].

$$\nabla \cdot \boldsymbol{\tau}(\mathbf{u}, \mathbf{u}) \approx -\nabla \cdot (\nu_T \nabla^s \bar{\mathbf{u}}) + \text{terms incorporated into } \bar{p},$$

where $\nabla^s \bar{\mathbf{u}}$ is the deformation tensor and $\nu_T \geq 0$ is the “turbulent viscosity coefficient”. The most common EV model is known in LES as the *Smagorinsky model* [33,

^{*}Department of Mathematics, Virginia Polytechnic Institute and State University, 528 McBryde Hall, Blacksburg, VA 24061, U.S.A., (borggaard@vt.edu); partially supported by AFOSR grants F49620-00-1-0299, F49620-03-1-0243, and FA9550-05-1-0449 and NSF grants DMS-0322852 and DMS-0513542.

[†]Department of Mathematics, Virginia Polytechnic Institute and State University, 456 McBryde Hall, Blacksburg, VA 24061, U.S.A., (iliescu@math.vt.edu); partially supported by AFOSR grants F49620-03-1-0243, and FA9550-05-1-0449 and NSF grants DMS-0209309, DMS-0322852, and DMS-0513542.

[‡]Department of Mathematics, Virginia Polytechnic Institute and State University, 528 McBryde Hall, Blacksburg, VA 24061, U.S.A., (jroop@math.vt.edu); partially supported by AFOSR grant F49620-00-1-0299 .

34, 37, 49, 53] in which

$$\nu_T = \nu_{\text{Smag}}(\bar{\mathbf{u}}, \delta) := (c_s \delta)^2 \|\nabla^s \bar{\mathbf{u}}\|_F. \quad (1.1)$$

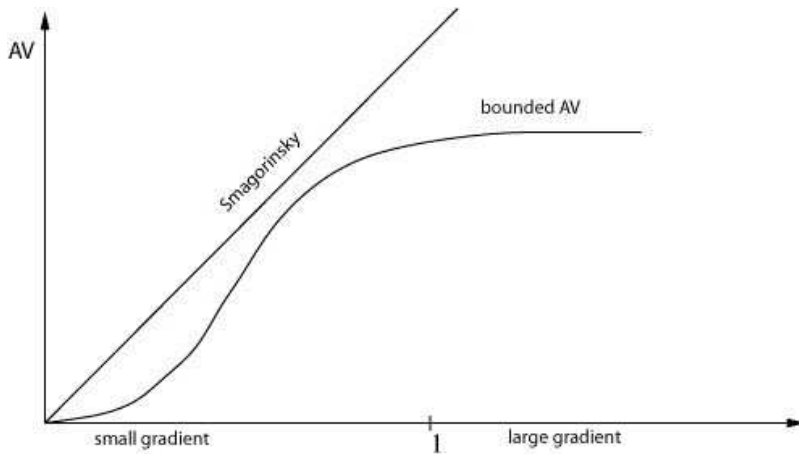


Figure 1: The amount of artificial viscosity introduced by the Smagorinsky and the bounded AV models against $\|\delta \nabla^s \bar{\mathbf{u}}\|$.

Although the Smagorinsky model is easy to implement, stable, and replicates energy dissipation rates, it is quite inaccurate for many problems. Probably the most common complaint for the Smagorinsky model (1.1) is that it is *too dissipative*. The reason is clearly illustrated in Figure 1: for large values of the velocity deformation tensor, the Smagorinsky model introduces an unbounded amount of artificial viscosity (AV). This behavior is manifest in practical computations of flows displaying large velocity deformation tensors, such as wall-bounded flows. For example, for turbulent channel flows and pipe flows [42], the Smagorinsky model yields unphysical results.

Different approaches have been devised to cope with this limitation: the “clipping procedure” [2, 10, 11, 23, 32, 54], the van Driest damping [6, 28, 29, 42, 52], the *Ri*-dependent Smagorinsky model [14, 18, 38, 46, 48, 50] (where *Ri* is the Richardson number, the square of the ratio of the buoyancy frequency and the vertical shear), the dynamic SGS model [22], and the Lagrangian dynamic SGS model [39, 43]. All of these approaches target the same deficiency of the Smagorinsky model – its overly diffusive character.

In this paper, we consider a *bounded artificial viscosity model* for the numerical simulation of turbulent flows with high velocity deformation tensors. The bounded AV model has a *general* form: it can be used to reduce the overly dissipative nature of the Smagorinsky model without massive *a priori* knowledge of the flow regime. The bounded AV model reads

$$\nu_T = \mu \delta^\sigma a(\delta \|\nabla^s \bar{\mathbf{u}}\|_F) \nabla^s \bar{\mathbf{u}}, \quad (1.2)$$

where $a(\cdot)$ is a general function whose graph resembles that in Figure 1.

The bounded AV model was proposed in [27] as an alternative to the Smagorinsky model and yielded improved results for convection-dominated convection-diffusion problems. In this paper, we analyze and test the bounded AV model (1.2) in the numerical simulation of incompressible fluid flows.

The paper is organized as follows: In Section 2, we discuss the commonly used eddy viscosity model. We note the benefits and limitations of heuristic procedures in which a “clipping” of the Smagorinsky artificial viscosity is performed, and present (1.2) as a viable alternative to such strategies. In Section 3, we provide the variational setting for which the NSE with (1.2) is solved and introduce the necessary notations. In Section 4, we present some stability results for the variational solution to NSE with (1.2), which are generalizations of Leray’s inequality for the usual Navier-Stokes system. In Section 5, we prove an error estimate for the semi-discrete finite element approximation of NSE with (1.2). Finally, in Section 6, we include finite element calculations for NSE with (1.2) which both support the theoretical error estimate of Section 6, and show that the bounded AV model (1.2) yields better results than the Smagorinsky model (1.1) in the numerical simulation of channel flows. We provide both sequential computations for an academic vortex decay problem and parallel computations for a 3D channel flow, using the Virginia Tech Large Eddy Simulator (ViTLES).

2. Large Eddy Simulation. LES is connected to a natural computational idea: when a computational mesh is so coarse that the problem data and solution sought fluctuate significantly inside each mesh cell, it is only reasonable to replace the problem data by mesh cell averages of that data and for the approximate solution to represent a mesh cell average of the true solution. Thus, if δ is the mesh cell width, then we should seek to approximate not the pointwise fluid velocity $\mathbf{u}(\mathbf{x}, t)$ but rather some mesh cell average $\overline{\mathbf{u}}(\mathbf{x}, t)$. The simplest such average is given by the convolution of the velocity \mathbf{u} with a rapidly decaying spatial filter $g_\delta(\mathbf{x})$. The filters $g_\delta(\mathbf{x})$ most commonly used are the sharp cut-off, box (top hat), Gaussian, and differential.

Then this is the idea of LES in a nutshell: pick a useful filter $g_\delta(\mathbf{x})$ and define $\overline{\mathbf{u}}(\mathbf{x}, t) := (g_\delta * \mathbf{u})(\mathbf{x}, t)$. Derive appropriate equations for $\overline{\mathbf{u}}$ by filtering the Navier-Stokes equations (NSE). Solve the closure problem. Impose accurate boundary conditions for $\overline{\mathbf{u}}$. Then discretize the resulting continuum model and solve it. Generally, such an averaging suppresses any fluctuations in \mathbf{u} below $O(\delta)$ and preserves those on scales larger than $O(\delta)$.

In many flows, the portion of the flow that must be modeled, $\mathbf{u}' := \mathbf{u} - \overline{\mathbf{u}}$, is small relative to the portion that is calculated, $\overline{\mathbf{u}}$. Models in LES tend to be both simple and accurate, and the overall computational cost tends not to be much greater than doing an (unreliable, under-refined) solution of the NSE on the same mesh.

In the case of an incompressible fluid, the non-dimensionalized form of the Navier-Stokes equations (NSE) is

$$\mathbf{u}_t - Re^{-1} \Delta \mathbf{u} + (\mathbf{u} \cdot \nabla) \mathbf{u} + \nabla p = \mathbf{f}, \quad \text{in } \Omega, \quad (2.1)$$

$$\nabla \cdot \mathbf{u} = 0, \quad \text{in } \Omega, \quad (2.2)$$

$$\mathbf{u} = 0, \quad \text{on } \partial\Omega. \quad (2.3)$$

where \mathbf{u} is the velocity, p is the pressure, and $Re := UL/\nu$ is the Reynolds number, defined as the ratio between the product of a characteristic length-scale L and a characteristic velocity U , and the kinematic viscosity ν .

To derive equations for $\overline{\mathbf{u}}$, we convolve the NSE with the chosen filter function $g_\delta(\mathbf{x})$. Using the fact that (for constant $\delta > 0$ and in the absence of boundaries) filtering commutes with differentiation, gives the space-filtered NSE:

$$\overline{\mathbf{u}}_t - Re^{-1} \Delta \overline{\mathbf{u}} + \nabla \cdot (\overline{\mathbf{u} \mathbf{u}^T}) + \nabla \overline{p} = -\nabla \cdot \boldsymbol{\tau}(\mathbf{u}, \mathbf{u}) \quad \text{in } \Omega \times (0, T), \quad (2.4)$$

$$\nabla \cdot \overline{\mathbf{u}} = 0 \quad \text{in } \Omega \times (0, T). \quad (2.5)$$

This system is not closed, since it involves both \mathbf{u} and $\overline{\mathbf{u}}$. The tensor $\boldsymbol{\tau}(\mathbf{u}, \mathbf{u}) = \overline{\mathbf{u} \mathbf{u}^T} - \overline{\mathbf{u}} \overline{\mathbf{u}}^T$ or $\tau_{ij}(\mathbf{u}, \mathbf{u}) = \overline{u_i u_j} - \overline{u_i} \overline{u_j}$ is often called the subgrid-scale stress (SGS) tensor. Thus, the closure problem in LES is to model the SGS tensor $\boldsymbol{\tau}(\mathbf{u}, \mathbf{u})$, i.e. to specify a tensor $\mathcal{S} = \mathcal{S}(\overline{\mathbf{u}}, \overline{\mathbf{u}})$ to replace $\boldsymbol{\tau}(\mathbf{u}, \mathbf{u})$ in (2.4).

2.1. Eddy Viscosity Models. The most popular approach to the closure problem is the Eddy Viscosity (EV) model. EV models are motivated by the idea that the global effect of the subfilter-scale stress tensor $\boldsymbol{\tau}(\mathbf{u}, \mathbf{u})$, in the mean, is to transfer energy from resolved to unresolved scales through inertial interactions. EV models are motivated by Kolmogorov’s (K-41) theory ([19, 42, 47]), and in particular by the *energy cascade*. The essence of the energy cascade ([45]) is that kinetic energy enters the turbulent flow at the largest scales of motion, and is then transferred by inviscid processes to smaller and smaller scales, until it is eventually dissipated through viscous effects. Thus, the action of the subfilter-scale stress $\boldsymbol{\tau}$ is thought of as having a dissipative effect on the mean flow: the scales uncaptured on the numerical mesh (above the cut-off wavenumber k_c) should dissipate energy from the large scales (below the cut-off wavenumber k_c).

Boussinesq [7] first formulated the *EV/Boussinesq hypothesis* based upon an analogy between the interaction of small eddies and the perfectly elastic collision of molecules (e.g., molecular viscosity or heat): “*Turbulent fluctuations are dissipative in the mean.*” The mathematical realization is the model

$$\nabla \cdot \boldsymbol{\tau}(\mathbf{u}, \mathbf{u}) \approx -\nabla \cdot (\nu_T \nabla^s \overline{\mathbf{u}}) + \text{terms incorporated into } \overline{p},$$

where $\nabla^s \overline{\mathbf{u}} := (\nabla \overline{\mathbf{u}} + \nabla \overline{\mathbf{u}}^T)/2$ is the deformation tensor of $\overline{\mathbf{u}}$ and $\nu_T \geq 0$ is the “turbulent viscosity coefficient”. The modeling problem then reduces to determining one parameter: the turbulent viscosity coefficient $\nu_T(\overline{\mathbf{u}}, \delta)$.

2.2. The Smagorinsky Model. The most common EV model is known in LES as the Smagorinsky model, in which

$$\nu_T = \nu_{\text{Smag}}(\overline{\mathbf{u}}, \delta) := (c_s \delta)^2 \|\nabla^s \overline{\mathbf{u}}\|_F, \quad (2.6)$$

where δ is the filter radius, c_s is the Smagorinsky constant, and $\|\sigma\|_F := \sqrt{\sum_{i,j=1}^d |\sigma_{ij}|^2}$ is the Frobenius norm of the tensor σ . This model was studied in [53] as a nonlinear artificial viscosity in gas dynamics and in [49] for geophysical flow calculations. A complete mathematical theory for partial differential equations involving this term was constructed by Ladyžhenskaya [33, 34].

The Smagorinsky model (1.1) where $c_s \sim 0.17$ [37] seems to be a universal answer in LES. It is easy to implement, stable, and (under “optimistic” assumptions) it replicates energy dissipation rates. Unfortunately, it can be also quite inaccurate for many problems.

The most successful form of the Smagorinsky model is the *dynamic* SGS model of [22], in which c_s is chosen locally in space and time, $c_s = c_s(\mathbf{x}, t)$. An essential improvement is that the dynamic SGS model introduces *backscatter* ([41]), the inverse transfer of energy from small scales to large scales [29, 6]. A yet improved version of the dynamic SGS model is the *Lagrangian dynamic* SGS model of [39, 43].

2.3. The Overly Diffusive Character of the Smagorinsky Model. Whether simplistic or more involved, all these approaches target the same deficiency of the Smagorinsky model - its overly diffusive character. This negative feature of the Smagorinsky model is clearly illustrated by the schematic in Figure 1. Plotting the

amount of AV introduced by the Smagorinsky model against $\|\delta \nabla^s \bar{\mathbf{u}}\|$, we obtain a linear profile: Indeed, (1.1) can be rewritten as

$$\nu_T = \nu_{\text{Smag}}(\bar{\mathbf{u}}, \delta) = c_s^2 \delta \|\delta \nabla^s \bar{\mathbf{u}}\|_F, \quad (2.7)$$

which yields a linear profile for ν_T (if δ is held constant). In smooth regions of the flow, where the deformation tensor is relatively small ($\|\nabla^s \bar{\mathbf{u}}\|_F \leq O(1/\delta)$), the Smagorinsky model will introduce a moderate amount of AV ($\nu_T \leq O(\delta)$). In those regions of the flow where the deformation tensor is large ($\|\nabla^s \bar{\mathbf{u}}\|_F \geq O(1/\delta^2)$, for example), the Smagorinsky model will introduce an *unphysical* amount of AV ($\nu_T \sim O(1)$).

The overly diffusive feature of the Smagorinsky model is manifest in practical computations of flows displaying a large deformation tensor, such as wall-bounded flows. Indeed, for turbulent channel flows and pipe flows, because the velocity deformation tensor is very large near the solid wall, the Smagorinsky model introduces an unphysical amount of AV. Similarly, in stratified flows with large shear (and thus, large deformation tensors), the Smagorinsky model introduces an unphysical amount of AV in the vertical direction.

There have been numerous modifications of the Smagorinsky model, all trying to attenuate its overly diffusive character. The simplest such approach is the “clipping procedure”

$$\nu_T = \nu_{\text{Smag}}^{\text{clipping}}(\bar{\mathbf{u}}, \delta) := \min\{\nu_{\text{Smag}}(\bar{\mathbf{u}}, \delta), C\}, \quad (2.8)$$

where C is a user-defined constant [2, 10, 11, 23, 32, 54].

A more involved approach for wall-bounded flows (such as channel and pipe flows) is the Van Driest damping [6, 28, 29, 42, 52], in which

$$\nu_T = \nu_{\text{Smag}}^{\text{VD}}(\bar{\mathbf{u}}, \delta) := \left[\left(1 - e^{-\frac{y^+}{25}} \right) \right] \nu_{\text{Smag}}(\bar{\mathbf{u}}, \delta), \quad (2.9)$$

where y^+ is the nondimensionalized distance to the wall (see Chapter 12 in [6] for more details). The main improvement over the *ad hoc* clipping procedure (2.8) is that the damping function in (2.9) is chosen so that the resulting flow satisfy the turbulent boundary layer theory [42].

In stratified flows, the Smagorinsky model is used with a damping function in the vertical direction [14, 18, 38, 46, 48, 50]

$$\nu_T^z = \nu_{\text{Smag}}^{\text{Ri}}(\bar{\mathbf{u}}, \delta) := \sqrt{1 - \frac{\text{Ri}}{\text{Ri}_c}} \nu_{\text{Smag}}(\bar{\mathbf{u}}, \delta), \quad (2.10)$$

where Ri is the Richardson number, the square of the ratio of the buoyancy frequency and the vertical shear, and Ri_c is a critical Richardson number (a popular choice is $\text{Ri}_c \sim 0.25$) [40, 46].

2.4. The Bounded AV Model. We consider in this paper the bounded AV model, a general, mathematically sound alternative to the Smagorinsky model. The bounded AV model reads

$$\nu_T = \mu \delta^\sigma a(\delta \|\nabla^s \bar{\mathbf{u}}\|_F) \nabla^s \bar{\mathbf{u}}, \quad (2.11)$$

where $a(\cdot)$ is a general function whose graph resembles that in Figure 1. This new model, proposed in [27] for convection-diffusion problems, is a clear improvement over

the Smagorinsky model. Indeed, in the flow regions with large velocity deformation tensors, the bounded AV model introduces a *bounded* amount of AV, just enough to spread the solution onto the computational mesh. This is in clear contrast with the Smagorinsky model, which introduces an unbounded amount of AV, thus being overly dissipative. The improvement of the bounded AV model over the Smagorinsky model is clearly supported by the 3D channel flow experiment in Section 7.

Another distinct advantage that the bounded AV model possesses over other modifications of the Smagorinsky model is that, when appropriately chosen, the bounded AV term represents a monotonic semi-linear operator. This property allows for the existence and uniqueness results as well as the error estimates presented herein. It is important to note that the results of this paper are very difficult to obtain for the previously mentioned heuristic AV bounding techniques.

The bounded AV model is general. Indeed, the function $a(\cdot)$ in (1.2) is just required to be bounded and monotonically increasing (see Figure 1). Thus, the bounded AV model clearly includes as a particular case the *ad hoc* “clipped” Smagorinsky model (2.8). Although the bounded AV model does not directly include the Smagorinsky model with Van Driest damping (2.9) ($a(\cdot)$ must be monotonically increasing) or the *Ri*-dependent Smagorinsky model (2.10) ($a(\cdot)$ depends on $\nabla^s \mathbf{u}$, whereas (2.10) depends on $\frac{\partial \mathbf{u}}{\partial z}$), it is certainly related to these two models, targeting the overly diffusive character of the Smagorinsky model. Note also that, while models (2.9) and (2.10) are tailored for specific flows (wall-bounded and stratified, respectively), the bounded AV model is not restricted to any particular type of flow.

It was shown in [27] that the bounded AV model yields a clear improvement over the Smagorinsky model in the numerical simulation of convection-dominated convection-diffusion problems with sharp transition layers. In this paper, we show that the bounded AV model is a dramatic improvement over the Smagorinsky model in the numerical simulation of a 3D channel flow.

There are numerous challenges in the numerical analysis of LES, where the study of classic topics such as consistency, stability, and convergence of the LES discretization are still at an initial stage. Only the first few steps along these lines have been made, some of which are presented in the exquisite monograph of John [30]. A thorough numerical analysis for the finite element implementation of the Smagorinsky model has been presented in [15, 16]. Further studies have been presented in [35]. In [31], the authors have presented a rigorous numerical analysis for the popular claim that the Smagorinsky model yields error estimates which are independent of the Re .

In this paper, we present a rigorous numerical analysis for the finite element implementation of the bounded AV model:

$$\mathbf{w}_t - Re^{-1} \Delta \mathbf{w} - \nabla \cdot (\mu \delta^\sigma a(\delta \|\nabla^s \mathbf{w}\|_F) \nabla^s \mathbf{w}) + (\mathbf{w} \cdot \nabla) \mathbf{w} - \nabla q = \bar{\mathbf{f}} \text{ in } \Omega, \quad (2.12)$$

$$\nabla \cdot \mathbf{w} = 0 \text{ in } \Omega, \quad (2.13)$$

$$\mathbf{w} = 0 \text{ on } \partial\Omega. \quad (2.14)$$

We also illustrate our error estimates through numerical simulations with the bounded AV model for the 3D channel flow and the 2D vortex decay problem.

REMARK 2.1. *The numerical analysis presented herein is concerned with the numerical error (i.e., $\mathbf{w} - \mathbf{w}_h$) associated with the bounded AV model, and not the modeling error (i.e., $\bar{\mathbf{u}} - \mathbf{w}$) associated with the proposed eddy-viscosity model.*

3. The Variational Formulation. In this section, we develop the variational formulation for (2.12)-(2.14). We will denote by $W^{m,p}(\Omega)$ the usual Sobolev spaces

[1] with norms $\|\cdot\|_{W^{m,p}}$ and semi-norms $|\cdot|_{W^{m,p}}$, and set $H^m(\Omega) := W^{m,2}(\Omega)$ and $L^p(\Omega) := W^{0,p}(\Omega)$. In the sequel we will denote $\|\cdot\|$ and (\cdot, \cdot) the norm and inner product for $L^2(\Omega)$, and $\|\cdot\|_m$ the norm for $H^m(\Omega)$.

Specifically, we use the following function spaces for the variational formulation:

$$\text{Velocity space : } \mathbf{X} := \mathbf{H}_0^1(\Omega) := \{ \mathbf{v} \in \mathbf{H}^1(\Omega) : \mathbf{v} = 0 \text{ on } \partial\Omega \},$$

$$\text{Pressure space : } Q := L_0^2(\Omega) := \left\{ q \in L^2(\Omega) : \int_{\Omega} q \, dx = 0 \right\}.$$

The variational formulation of (2.12)-(2.14) proceeds in the usual manner. Multiplying (2.12), (2.13) by a velocity (\mathbf{v}) and pressure (λ) test function, respectively, integrating over Ω , and integrating by parts (using the fact that $\mathbf{v} = 0$ on $\partial\Omega$), we obtain

$$\begin{aligned} (\mathbf{w}_t, \mathbf{v}) + A(\mathbf{w}, \mathbf{v}) + B(\mathbf{w}, \mathbf{w}, \mathbf{v}) \\ + C(\mathbf{w}, \mathbf{w}, \mathbf{v}) - (q, \nabla \cdot \mathbf{v}) = (\bar{\mathbf{f}}, \mathbf{v}), \quad \forall \mathbf{v} \in \mathbf{X}, \quad t \in [0, T], \end{aligned} \quad (3.1)$$

$$(\nabla \cdot \mathbf{w}, \lambda) = 0, \quad \forall \lambda \in Q, \quad t \in [0, T] \quad (3.2)$$

where the bilinear form $A(\cdot, \cdot)$ is defined by

$$A(\mathbf{w}, \mathbf{v}) := Re^{-1} (\nabla \mathbf{w}, \nabla \mathbf{v}),$$

and the trilinear forms $B(\cdot, \cdot, \cdot)$ and $C(\cdot, \cdot, \cdot)$ are defined by

$$B(\mathbf{u}, \mathbf{v}, \mathbf{w}) := \mu \delta^\sigma (a(\delta \|\nabla \mathbf{u}\|_F) \nabla \mathbf{v}, \nabla \mathbf{w}),$$

$$C(\mathbf{u}, \mathbf{v}, \mathbf{w}) := (\mathbf{u} \cdot \nabla \mathbf{v}, \mathbf{w}).$$

REMARK 3.1. *Although the bounded AV model (2.12)-(2.14) depends on $\nabla^s \mathbf{w}$, for clarity we will replace $\nabla^s \mathbf{w}$ by $\nabla \mathbf{w}$. The same numerical analysis can be carried out with the $\nabla^s \mathbf{w}$ by using Korn's inequalities, which relates the L^p -norms of the deformation tensor $\nabla^s \mathbf{w}$ to the same norms of the gradient $\nabla \mathbf{w}$ for $1 < p < \infty$ [21, 31].*

In addition, note that the velocity and pressure spaces, \mathbf{X} and Q , satisfy the *inf-sup* condition [24].

$$\inf_{\lambda \in Q} \sup_{\mathbf{v} \in \mathbf{X}} \frac{(\lambda, \nabla \cdot \mathbf{v})}{\|\lambda\| \|\mathbf{v}\|_1} \geq \beta > 0. \quad (3.3)$$

The *inf-sup* condition (3.3), in turn, implies that the space of weakly divergence-free functions \mathbf{V} ,

$$\mathbf{V} := \{ \mathbf{v} \in \mathbf{X} : (\lambda, \nabla \cdot \mathbf{v}) = 0, \quad \forall \lambda \in Q \}, \quad (3.4)$$

is a well defined, nontrivial, closed subspace of \mathbf{X} [24].

3.1. Finite Element Spaces. Let $\Omega \subset \mathbb{R}^d$, ($d = 2, 3$) be a polygonal domain and let T_h denote a triangulation of Ω made up of triangles (in \mathbb{R}^2) or tetrahedrons (in \mathbb{R}^3). Thus, the computational domain is defined by

$$\Omega = \bigcup K, \quad K \in T_h.$$

We also assume that for a particular triangulation T_h of Ω , there exist constants c_1, c_2 such that

$$c_1 h \leq h_K \leq c_2 \rho_K,$$

where h_K is the diameter of K , ρ_K is the diameter of the greatest ball (sphere) included in K and $h = \max_{K \in T_h} h_K$. Let $P_K(A)$ denote the space of polynomials on A of degree no greater than k . Then we define the conforming finite element spaces associated with the velocity and pressure spaces as follows:

$$\begin{aligned} \mathbf{X}_h &:= \{ \mathbf{v}_h \in \mathbf{X} \cap C(\bar{\Omega})^d : \mathbf{v}_h|_K \in P_k(K), \forall K \in T_h \}, \\ Q_h &:= \{ \lambda_h \in Q \cap C(\bar{\Omega}) : \lambda_h|_K \in P_q(K), \forall K \in T_h \}, \end{aligned}$$

where $C(\bar{\Omega})$ denotes the set of continuous functions on the closure of Ω . Analogous to the continuous *inf-sup* condition, we also assume that the spaces \mathbf{X}_h, Q_h satisfy the *discrete inf-sup* condition [17, 24]

$$\inf_{\lambda_h \in Q_h} \sup_{\mathbf{v}_h \in \mathbf{X}_h} \frac{(\lambda_h, \nabla \cdot \mathbf{v}_h)}{\|\lambda_h\| \|\mathbf{v}_h\|_1} \geq \beta > 0. \quad (3.5)$$

The *discrete inf-sup* condition (3.3), in turn, implies that the space of weakly divergence-free functions \mathbf{V}_h ,

$$\mathbf{V}_h := \{ \mathbf{v}_h \in \mathbf{X}_h : (\lambda_h, \nabla \cdot \mathbf{v}_h) = 0, \forall \lambda_h \in Q_h \}, \quad (3.6)$$

is a well defined, nontrivial, closed subspace of \mathbf{X}_h [17, 24, 25].

We now note the usual approximation properties for the finite element spaces \mathbf{X}_h, Q_h . For $(\mathbf{w}, \lambda) \in \mathbf{H}^{k+1}(\Omega) \times H^{q+1}(\Omega)$, we have that there exist interpolants $(I_h \mathbf{w}, I_h \lambda) \in \mathbf{X}_h \times Q_h$ satisfying [8, 24]

$$\|\mathbf{w} - I_h \mathbf{w}\| \leq C_I h^{k+1} |\mathbf{w}|_{\mathbf{H}^{k+1}}, \quad (3.7)$$

$$\|\mathbf{w} - I_h \mathbf{w}\|_1 \leq C_I h^k |\mathbf{w}|_{\mathbf{H}^{k+1}}, \quad (3.8)$$

$$\|\lambda - I_h \lambda\| \leq C_I h^q |\lambda|_{H^{q+1}}. \quad (3.9)$$

From [8], we have the following useful results concerning interpolation:

LEMMA 3.1. *Let $\{T_h\}$ ($0 < h \leq 1$) denote a quasi-uniform family of subdivisions of a polyhedral domain $\Omega \subset \mathbb{R}^d$. Let (\hat{K}, P, N) be a reference finite element such that $P \subset W^{l,p}(\hat{K}) \cap W^{m,q}(\hat{K})$ where $1 \leq p, q \leq \infty$ and $0 \leq m \leq l$. For $K \in T_h$, let (K, P_K, N_K) be the affine equivalent element and*

$$V_h := \left\{ v : v \text{ is measurable and } v|_K \in P_K, \forall K \in T_h \right\}.$$

Then there exists $C = C(l, p, q)$ such that

$$\left[\sum_{K \in T_h} \|v\|_{W^{l,p}(K)}^p \right]^{1/p} \leq C h^{m-l+\min(0, \frac{d}{p}-\frac{d}{q})} \left[\sum_{K \in T_h} \|v\|_{W^{m,q}(K)}^q \right]^{1/q}. \quad (3.10)$$

The following result proves useful in bounding the L^∞ and $W^{1,\infty}$ norms for the piecewise polynomial interpolants of \mathbf{w} .

LEMMA 3.2. *Let $I_h v$ denote the interpolant of v . Then for all $v \in W^{m,p}(\Omega) \cap C^r(\Omega)$ and $0 \leq s \leq \min\{m, r+1\}$,*

$$\|v - I_h v\|_{W^{s,\infty}} \leq C h^{m-s-d/p} |v|_{W^{m,p}}.$$

4. Stability Results. In this section, we prove some stability results concerning the variational problem (3.1)-(3.2), as well as its semi-discrete finite element approximation. Useful in the following analysis are the following three lemmas:

LEMMA 4.1. (*Monotonicity of $B(\cdot, \cdot, \cdot)$ [27].*) For $\mathbf{u}, \mathbf{v} \in \mathbf{X}$, and the function $a(\cdot)$ satisfying

$$0 \leq a(x) \leq 1, \quad a'(x) \geq 0, \quad \forall x \in [0, \infty),$$

we have

$$B(\mathbf{u}, \mathbf{u}, \mathbf{u} - \mathbf{v}) - B(\mathbf{v}, \mathbf{v}, \mathbf{u} - \mathbf{v}) \geq 0$$

Proof. Consider the functional $I : \mathbf{X} \rightarrow \mathbb{R}$, defined by

$$I(\mathbf{U}) := \int_{\Omega} A(\|\nabla \mathbf{U}\|_F) \, d\mathbf{x},$$

where the function $A : [0, \infty) \rightarrow \mathbb{R}$ is defined by

$$A(x) := \int_0^x t a(t) \, dt.$$

First, note that

$$dI(\mathbf{U}, \mathbf{V}) = \int_{\Omega} A'(\|\mathbf{U}\|_F) \frac{\nabla \mathbf{U}}{\|\nabla \mathbf{U}\|_F} \nabla \mathbf{V} \, d\mathbf{x} = \int_{\Omega} a(\|\nabla \mathbf{U}\|_F) \nabla \mathbf{U} \nabla \mathbf{V} \, d\mathbf{x},$$

where $dI(\mathbf{U}, \mathbf{V})$ is the Gâteaux derivative of I at \mathbf{U} in the direction of \mathbf{V} .

Therefore, setting $\mathbf{U}_1 := \delta \mathbf{u}$, $\mathbf{U}_2 := \delta \mathbf{v}$, and $\mathbf{V} := \mathbf{U}_1 - \mathbf{U}_2$, we have

$$B(\mathbf{u}, \mathbf{u}, \mathbf{u} - \mathbf{v}) - B(\mathbf{v}, \mathbf{v}, \mathbf{u} - \mathbf{v}) = \frac{\mu \delta^\sigma}{\delta^2} (dI(\mathbf{U}_1, \mathbf{V}) - dI(\mathbf{U}_2, \mathbf{V})). \quad (4.1)$$

However, we can rewrite this expression as

$$\begin{aligned} dI(\mathbf{U}_1, \mathbf{V}) - dI(\mathbf{U}_2, \mathbf{V}) &= \int_0^1 \frac{d}{dt} dI(\mathbf{U}_2 + t(\mathbf{U}_1 - \mathbf{U}_2), \mathbf{V}) \, dt \\ &= \int_0^1 \frac{d}{dt} \int_{\Omega} a(\|\nabla(\mathbf{U}_2 + t(\mathbf{U}_1 - \mathbf{U}_2))\|_F) \nabla(\mathbf{U}_2 + t(\mathbf{U}_1 - \mathbf{U}_2)) \nabla \mathbf{V} \, d\mathbf{x} \, dt \\ &= \int_0^1 \int_{\Omega} a'(\|\nabla(\mathbf{U}_2 + t(\mathbf{U}_1 - \mathbf{U}_2))\|_F) \frac{\nabla(\mathbf{U}_2 + t(\mathbf{U}_1 - \mathbf{U}_2)) \nabla \mathbf{V}}{\|\nabla(\mathbf{U}_2 + t(\mathbf{U}_1 - \mathbf{U}_2)) \nabla \mathbf{V}\|_F} \\ &\quad \nabla(\mathbf{U}_2 + t(\mathbf{U}_1 - \mathbf{U}_2)) \nabla \mathbf{V} \, d\mathbf{x} \, dt \\ &\quad + \int_0^1 \int_{\Omega} a(\|\nabla(\mathbf{U}_2 + t(\mathbf{U}_1 - \mathbf{U}_2))\|_F) \|\nabla \mathbf{V}\|_F^2 \, d\mathbf{x} \, dt. \end{aligned} \quad (4.2)$$

As $a(x), a'(x) \geq 0$, it is clear that the expression in (4.2) is nonnegative. Finally, using (4.1) we obtain the stated result. \blacksquare

REMARK 4.1. Notice that Lemma 4.1 states that the bounded AV operator $B(\cdot, \cdot, \cdot)$ is monotone, but not strongly monotone. The Smagorinsky AV operator

$$B^{Smag}(\mathbf{u}, \mathbf{v}, \mathbf{w}) := ((c_s \delta)^2 \|\nabla^s \mathbf{u}\|_F \nabla^s \mathbf{v}, \nabla^s \mathbf{w}),$$

on the other hand, is strongly monotone [16, 31, 35]. Indeed, $\forall \mathbf{u}, \mathbf{v} \in [W^{1,3}(\Omega)]^d$, $d = 2, 3$

$$B^{Smag}(\mathbf{u}, \mathbf{u}, \mathbf{u} - \mathbf{v}) - B^{Smag}(\mathbf{v}, \mathbf{v}, \mathbf{u} - \mathbf{v}) \geq C \delta^2 \|\nabla^s(\mathbf{u} - \mathbf{v})\|_{L^3}^3.$$

Therefore, the error estimate we prove in Theorem 5.1 for the bounded AV model assumes higher regularity for the solution \mathbf{w} ($\mathbf{w} \in L^4(0, T; \mathbf{W}^{1,\infty}(\Omega))$) than the regularity for \mathbf{w} assumed for the Smagorinsky model [31] ($\mathbf{w} \in L^2(0, T; \mathbf{W}^{1,\infty}(\Omega))$).

Note, however, that in the limit as $\delta \rightarrow 0$, the bounded AV model resembles the p -Laplacian. Indeed, if $\delta \rightarrow 0$, then $\|\delta \nabla \mathbf{u}\|_F \rightarrow 0$, and the function $a(\delta \|\nabla \mathbf{u}\|_F)$ in Figure 1 resembles the graph of the p -Laplacian.

LEMMA 4.2. For $\mathbf{u}_1, \mathbf{u}_2, \mathbf{v}, \mathbf{w} \in \mathbf{X}$, and the function $a(\cdot)$ satisfying

$$0 \leq a(x) \leq 1, \quad 0 \leq a'(x) \leq M_a, \quad \forall x \in [0, \infty),$$

we have

$$|B(\mathbf{u}_1, \mathbf{v}, \mathbf{w}) - B(\mathbf{u}_2, \mathbf{v}, \mathbf{w})| \leq M_a \mu \delta^{\sigma+1} (\|\nabla \mathbf{u}_1 - \nabla \mathbf{u}_2\|_F \|\nabla \mathbf{v}\|_F, \|\nabla \mathbf{w}\|_F) \quad (4.3)$$

and

$$|B(\mathbf{u}_1, \mathbf{v}, \mathbf{w})| \leq M_a \mu \delta^{\sigma+1} (\|\nabla \mathbf{u}_1\|_F \|\nabla \mathbf{v}\|_F, \|\nabla \mathbf{w}\|_F) \quad (4.4)$$

Proof. Without loss of generality, we assume that $\|\nabla \mathbf{u}_1\|_F \geq \|\nabla \mathbf{u}_2\|_F$. Immediately, we have

$$|B(\mathbf{u}_1, \mathbf{v}, \mathbf{w}) - B(\mathbf{u}_2, \mathbf{v}, \mathbf{w})| = \mu \delta^\sigma |([a(\delta \|\nabla \mathbf{u}_1\|_F) - a(\delta \|\nabla \mathbf{u}_2\|_F)] \nabla \mathbf{v}, \nabla \mathbf{w})|. \quad (4.5)$$

Now, by the mean value theorem, there exists $c_a \in [\delta \|\nabla \mathbf{u}_2\|_F, \delta \|\nabla \mathbf{u}_1\|_F]$, such that

$$a(\delta \|\nabla \mathbf{u}_1\|_F) - a(\delta \|\nabla \mathbf{u}_2\|_F) = a'(c_a) \delta (\|\nabla \mathbf{u}_1\|_F - \|\nabla \mathbf{u}_2\|_F).$$

Combining this with the reverse triangle inequality, $||x| - |y|| \leq |x - y|$, we have

$$|a(\delta \|\nabla \mathbf{u}_1\|_F) - a(\delta \|\nabla \mathbf{u}_2\|_F)| \leq a'(c_a) \delta \|\nabla \mathbf{u}_1 - \nabla \mathbf{u}_2\|_F. \quad (4.6)$$

Finally, substituting (4.6) into (4.5) and noting that $a'(c_a) \leq M_a$, we obtain (4.3). The result (4.4) follows directly. \blacksquare

REMARK 4.2. Again, the bounded AV operator $B(\cdot, \cdot, \cdot)$ satisfies a weaker inequality than the Smagorinsky AV operator $B^{Smag}(\cdot, \cdot, \cdot)$ [16, 31, 35].

LEMMA 4.3. (Leray's inequality for the bounded AV model.) A solution of (3.1)-(3.2) satisfies

$$\frac{1}{2} \|\mathbf{w}(t)\|^2 + \int_0^t R e^{-1} \|\nabla \mathbf{w}\|^2 dt' \leq \frac{1}{2} \|\mathbf{w}(0)\|^2 + \int_0^t (\mathbf{f}, \mathbf{w}) dt'.$$

Proof. The stated result follows by setting $\mathbf{v} = \mathbf{w}$ and $\lambda = q$ in (3.1) and (3.2), noting that

$$B(\mathbf{w}, \mathbf{w}, \mathbf{w}) \geq 0, \quad C(\mathbf{w}, \mathbf{w}, \mathbf{w}) = 0,$$

and integrating from 0 to t . \blacksquare

We now establish the semi-discrete approximation as the solution of (3.1)-(3.2) restricted to the finite element spaces \mathbf{X}_h, Q_h .

DEFINITION 4.4. (*The semi-discrete approximation.*) *The semi-discrete approximation is defined to be an element $(\mathbf{w}_h, q_h) \in C(0, T; \mathbf{X}_h) \cap C(0, T; Q_h)$ such that*

$$\begin{aligned} &(\mathbf{w}_{h,t}, \mathbf{v}_h) + A(\mathbf{w}_h, \mathbf{v}_h) + B(\mathbf{w}_h, \mathbf{w}_h, \mathbf{v}_h) \\ &+ C(\mathbf{w}_h, \mathbf{w}_h, \mathbf{v}_h) - (q_h, \nabla \cdot \mathbf{v}_h) = (\mathbf{f}, \mathbf{v}_h), \quad \forall \mathbf{v}_h \in \mathbf{X}_h, \quad t \in [0, T], \end{aligned} \quad (4.7)$$

$$(\nabla \cdot \mathbf{w}_h, \lambda_h) = 0, \quad \forall \lambda_h \in Q_h, \quad t \in [0, T]. \quad (4.8)$$

We immediately obtain the following two lemmas.

LEMMA 4.5. (*Leray's inequality for \mathbf{w}_h .*) *A solution of (4.7)-(4.8) satisfies*

$$\frac{1}{2} \|\mathbf{w}_h(t)\|^2 + \int_0^t Re^{-1} \|\nabla \mathbf{w}_h\|^2 dt' \leq \frac{1}{2} \|\mathbf{w}_h(0)\|^2 + \int_0^t (\mathbf{f}, \mathbf{w}_h) dt'.$$

Proof. Setting $\mathbf{v}_h = \mathbf{w}_h$ and $\lambda_h = q_h$ in (4.7)-(4.8), we immediately have

$$\frac{1}{2} \frac{d}{dt} \|\mathbf{w}_h(t)\|^2 + Re^{-1} \|\nabla \mathbf{w}_h\|^2 \leq (\mathbf{f}, \mathbf{w}_h). \quad (4.9)$$

Integrating from 0 to t thus yields the stated result. ■

LEMMA 4.6. (*Stability of \mathbf{w}_h .*) *A solution \mathbf{w}_h of (4.7)-(4.8) satisfies*

$$\begin{aligned} &\|\mathbf{w}_h(t)\|^2 + Re^{-1} C(\Omega) \int_0^t \|\mathbf{w}_h\|_{\mathbf{H}^1(\Omega)}^2 ds \\ &\leq \|\mathbf{w}_h(0)\|^2 + \frac{Re}{C(\Omega)} \int_0^t \|\bar{\mathbf{f}}\|_{\mathbf{H}^{-1}(\Omega)}^2 ds. \end{aligned} \quad (4.10)$$

$$\begin{aligned} &\|\mathbf{w}_h(t)\|^2 + 2Re^{-1} \int_0^t e^{t-s} \|\nabla \mathbf{w}_h\|^2 ds \\ &\leq e^t \|\mathbf{w}_h(0)\|^2 + \int_0^t e^{t-s} \|\bar{\mathbf{f}}\|^2 ds, \end{aligned} \quad (4.11)$$

where $C(\Omega)$ denotes a generic constant depending on Ω . Also, we have that $\mathbf{w}_h(t) \in L^\infty(\Omega)$ for all $t > 0$.

Proof. By using the Cauchy-Schwartz and Young's inequalities, we have

$$(\bar{\mathbf{f}}, \mathbf{w}_h) \leq \frac{\varepsilon}{2} \|\mathbf{w}_h\|_{\mathbf{H}^1(\Omega)}^2 + \frac{1}{2\varepsilon} \|\bar{\mathbf{f}}\|_{\mathbf{H}^{-1}(\Omega)}^2. \quad (4.12)$$

By using Poincaré's inequality [20], we get

$$Re^{-1} C(\Omega) \|\mathbf{w}_h\|_{\mathbf{H}^1(\Omega)}^2 \leq Re^{-1} \|\nabla \mathbf{w}_h\|^2. \quad (4.13)$$

Inserting (4.12) with $\varepsilon := Re^{-1} C(\Omega)$ and (4.12) in (4.9), we obtain

$$\frac{1}{2} \frac{d}{dt} \|\mathbf{w}_h\|^2 + \frac{Re^{-1} C(\Omega)}{2} \|\mathbf{w}_h\|_{\mathbf{H}^1(\Omega)}^2 \leq \frac{Re}{2 C(\Omega)} \|\bar{\mathbf{f}}\|_{\mathbf{H}^{-1}(\Omega)}^2. \quad (4.14)$$

By integrating (4.14) from 0 to t , we get (4.10).

By using the Cauchy-Schwartz and Young's inequalities, we have

$$(\bar{\mathbf{f}}, \mathbf{w}_h) \leq \frac{1}{2} \|\mathbf{w}_h\|^2 + \frac{1}{2} \|\bar{\mathbf{f}}\|^2. \quad (4.15)$$

By using (4.15) in (4.9), we obtain

$$\frac{1}{2} \frac{d}{dt} \|\mathbf{w}_h\|^2 - \frac{1}{2} \|\mathbf{w}_h\|^2 + Re^{-1} \|\nabla \mathbf{w}_h\|^2 \leq \frac{1}{2} \|\bar{\mathbf{f}}\|^2.$$

The positivity of the exponential implies

$$e^{-s} \left(\frac{d}{ds} \|\mathbf{w}_h\|^2 - \|\mathbf{w}_h\|^2 + 2 Re^{-1} \|\nabla \mathbf{w}_h\|^2 \right) \leq e^{-s} \|\bar{\mathbf{f}}\|^2.$$

By integrating from 0 to $t < T$ and then multiplying by e^t , we get (4.11). Finally, from (4.10) we have that

$$\|\nabla \mathbf{w}_h\| \leq C \|\mathbf{f}\|_{H^{-1}(\Omega)}.$$

The interpolation property (3.10) implies therefore, that

$$\|\mathbf{w}_h\|_{L^\infty(\Omega)} \leq Ch^{1-d/2} \|\bar{\mathbf{f}}\|_{H^{-1}(\Omega)}.$$

■

LEMMA 4.7. (*Existence of (\mathbf{w}_h, q_h) .*) *There exists a solution (\mathbf{w}_h, q_h) of the semi-discrete approximation (4.7)-(4.8).*

Proof. Since $\dim(\mathbf{X}_h) < \infty$ and any possible solution (\mathbf{w}_h, q_h) satisfies the *a priori* stability estimates in Lemma 4.6, Schauder's fixed point theorem [36] implies existence of a solution (\mathbf{w}_h, q_h) of the semi-discrete approximation (4.7)-(4.8). ■

REMARK 4.3. (*Uniqueness of (\mathbf{w}_h, q_h) .*) *The uniqueness of the solution (\mathbf{w}_h, q_h) of the semi-discrete approximation (4.7)-(4.8) would follow by using a general argument: Assume that there exist two distinct solutions $(\mathbf{w}_{1h}, q_{1h})$ and $(\mathbf{w}_{2h}, q_{2h})$ of (4.7)-(4.8); Subtract equations (4.7)-(4.8) corresponding to the two solutions; Use the coercivity of the operators in the error equation to obtain inequalities of the form $\|\mathbf{w}_{1h} - \mathbf{w}_{2h}\| \leq 0$ and $\|q_{1h} - q_{2h}\| \leq 0$.*

This approach fails for (4.7)-(4.8) because of the nonlinear term $C(\cdot, \cdot, \cdot)$ and the bounded AV operator $B(\cdot, \cdot, \cdot)$ being just monotone, and not strongly monotone (see Lemma 4.1).

Note, however, that when $\delta \rightarrow 0$, the bounded AV operator $B(\cdot, \cdot, \cdot)$ becomes strongly monotone (see Remark 4.1), which could in turn allow us to prove uniqueness of (\mathbf{w}_h, q_h) .

5. An *A Priori* Error Estimate. In order to prove an *a priori* error estimate for the semi-discrete approximation (\mathbf{w}_h, q_h) , we will assume that the solution to the continuous problem satisfies $\mathbf{w} \in L^4(0, T; \mathbf{W}^{1,\infty}(\Omega))$.

THEOREM 5.1. *Assume that the system (3.1)-(3.2) has a solution $(\mathbf{w}, q) \in \mathbf{X} \times Q$ which satisfies*

$$\mathbf{w} \in L^4(0, T; \mathbf{W}^{1,\infty}(\Omega)). \quad (5.1)$$

Let $b(t) := \frac{1}{2} + \frac{1}{2} \|\nabla \mathbf{w}\|_{\mathbf{L}^\infty}^2 + \|\nabla \mathbf{w}\|_{\mathbf{L}^\infty} + \frac{1}{2} \|\mathbf{w}\|_{\mathbf{L}^\infty}^2 + 2 Re^{-1} \|\mathbf{w}_h\|_{\mathbf{L}^\infty}^2$. Then, there is a constant $C_1 := C_1(\mathbf{w}, Re)$ such that

$$\|b(t)\|_{L^1(0, T)} \leq C_1(\mathbf{w}, Re). \quad (5.2)$$

Furthermore, the error $\mathbf{w} - \mathbf{w}_h$ satisfies for $T > 0$

$$\begin{aligned} & \|\mathbf{w} - \mathbf{w}_h\|_{L^\infty(0,T;L^2)}^2 + Re^{-1} \|\nabla(\mathbf{w} - \mathbf{w}_h)\|_{L^2(0,T;L^2)}^2 \\ & \leq C \exp(C_1(\mathbf{w}, Re)) \|(\mathbf{w} - \mathbf{w}_h)(\mathbf{x}, 0)\|^2 \\ & \quad + C \inf_{\tilde{\mathbf{w}} \in \mathbf{V}_h, \lambda_h \in Q_h} \mathcal{F}(\mathbf{w} - \tilde{\mathbf{w}}, q - \lambda_h, \delta, Re), \end{aligned} \quad (5.3)$$

where

$$\begin{aligned} & \mathcal{F}(\mathbf{w} - \tilde{\mathbf{w}}, q - \lambda_h, \delta, Re) \\ & := \|\mathbf{w} - \tilde{\mathbf{w}}\|_{L^\infty(0,T;L^2)}^2 + Re^{-1} \|\nabla(\mathbf{w} - \tilde{\mathbf{w}})\|_{L^2(0,T;L^2)}^2 \\ & \quad + C \exp(C_1(\mathbf{w}, Re)) \left[\|(\mathbf{w} - \tilde{\mathbf{w}})_t\|_{L^2(0,T;L^2)}^2 \right. \\ & \quad \left. + \|\mathbf{w} - \tilde{\mathbf{w}}\|_{L^2(0,T;L^2)}^2 + \|\nabla(\mathbf{w} - \tilde{\mathbf{w}})\|_{L^2(0,T;L^2)}^2 \right. \\ & \quad \left. + C(\Omega) \|\nabla(\mathbf{w} - \tilde{\mathbf{w}})\|_{L^4(0,T;L^2)}^2 + \|q - \lambda_h\|^2 \right]. \end{aligned}$$

Proof. First note that, for standard piecewise polynomial finite element spaces, it is known that the L^p -projection of a function in L^p , $p \geq 2$, is in L^p itself and the L^2 -projection operator is stable in L^p , $2 \leq p \leq \infty$ [12].

Let the error in \mathbf{w} be denoted by $\mathbf{e} := \mathbf{w} - \mathbf{w}_h$, and $\tilde{\mathbf{w}}$ denote a stable approximation of \mathbf{w} in \mathbf{V}_h , for example, the L^2 -projection under the conditions of [12].

The error \mathbf{e} is decomposed as

$$\mathbf{e} = (\mathbf{w} - \tilde{\mathbf{w}}) + (\tilde{\mathbf{w}} - \mathbf{w}_h) := \boldsymbol{\eta} + \boldsymbol{\phi}_h, \quad (5.4)$$

where $\boldsymbol{\eta} := \mathbf{w} - \tilde{\mathbf{w}}$ and $\boldsymbol{\phi}_h := \tilde{\mathbf{w}} - \mathbf{w}_h \in \mathbf{V}_h$. By subtracting (4.7) from (3.1) and using that $\mathbf{w} \in \mathbf{V}$, we obtain an error equation

$$\begin{aligned} & (\mathbf{e}_t, \mathbf{v}_h) + A(\mathbf{e}, \mathbf{v}_h) + [B(\mathbf{w}, \mathbf{w}, \mathbf{v}_h) - B(\mathbf{w}_h, \mathbf{w}_h, \mathbf{v}_h)] \\ & \quad + [C(\mathbf{w}, \mathbf{w}, \mathbf{v}_h) - C(\mathbf{w}_h, \mathbf{w}_h, \mathbf{v}_h)] - (q - \lambda_h, \nabla \cdot \mathbf{v}_h) = 0, \quad \forall (\mathbf{v}_h, \lambda_h) \in \mathbf{V}_h \times Q_h. \end{aligned} \quad (5.5)$$

By adding and subtracting terms, and setting $\mathbf{v}_h := \boldsymbol{\phi}_h$, (5.5) becomes

$$\begin{aligned} & (\boldsymbol{\phi}_{h,t}, \boldsymbol{\phi}_h) + A(\boldsymbol{\phi}_h, \boldsymbol{\phi}_h) + [B(\tilde{\mathbf{w}}, \tilde{\mathbf{w}}, \boldsymbol{\phi}_h) - B(\mathbf{w}_h, \mathbf{w}_h, \boldsymbol{\phi}_h)] \\ & \quad = -(\boldsymbol{\eta}_t, \boldsymbol{\phi}_h) - A(\boldsymbol{\eta}, \boldsymbol{\phi}_h) - [B(\mathbf{w}, \mathbf{w}, \boldsymbol{\phi}_h) - B(\tilde{\mathbf{w}}, \tilde{\mathbf{w}}, \boldsymbol{\phi}_h)] \\ & \quad \quad - [C(\mathbf{w}, \mathbf{w}, \boldsymbol{\phi}_h) - C(\mathbf{w}_h, \mathbf{w}_h, \boldsymbol{\phi}_h)] + (q - \lambda_h, \nabla \cdot \boldsymbol{\phi}_h). \end{aligned} \quad (5.6)$$

By using the monotonicity of $B(\cdot, \cdot, \cdot)$ (Lemma 4.1), we have

$$B(\tilde{\mathbf{w}}, \tilde{\mathbf{w}}, \boldsymbol{\phi}_h) - B(\mathbf{w}_h, \mathbf{w}_h, \boldsymbol{\phi}_h) \geq 0.$$

Thus, the left-hand side of (5.6) can be bounded from below as follows:

$$\begin{aligned} & (\boldsymbol{\phi}_{h,t}, \boldsymbol{\phi}_h) + A(\boldsymbol{\phi}_h, \boldsymbol{\phi}_h) + [B(\tilde{\mathbf{w}}, \tilde{\mathbf{w}}, \boldsymbol{\phi}_h) - B(\mathbf{w}_h, \mathbf{w}_h, \boldsymbol{\phi}_h)] \\ & \geq \frac{1}{2} \frac{d}{dt} \|\boldsymbol{\phi}_h\|^2 + Re^{-1} \|\nabla \boldsymbol{\phi}_h\|^2. \end{aligned} \quad (5.7)$$

We now start bounding from above the five terms on the right-hand side of (5.6). By using the Cauchy-Schwartz and Young's inequalities, we obtain

$$-(\boldsymbol{\eta}_t, \boldsymbol{\phi}_h) \leq |(\boldsymbol{\eta}_t, \boldsymbol{\phi}_h)| \leq \frac{1}{2} \|\boldsymbol{\phi}_h\|^2 + \frac{1}{2} \|\boldsymbol{\eta}_t\|^2, \quad (5.8)$$

$$-A(\boldsymbol{\eta}, \boldsymbol{\phi}_h) \leq |A(\boldsymbol{\eta}, \boldsymbol{\phi}_h)| \leq Re^{-1} \varepsilon_1 \|\nabla \boldsymbol{\phi}_h\|^2 + \frac{Re^{-1}}{4\varepsilon_1} \|\nabla \boldsymbol{\eta}\|^2. \quad (5.9)$$

By adding and subtracting terms and using Lemma 4.2, we get

$$\begin{aligned}
& B(\mathbf{w}, \mathbf{w}, \phi_h) - B(\tilde{\mathbf{w}}, \tilde{\mathbf{w}}, \phi_h) \leq |B(\mathbf{w}, \mathbf{w}, \phi_h) - B(\tilde{\mathbf{w}}, \tilde{\mathbf{w}}, \phi_h)| \\
& \leq |B(\mathbf{w}, \mathbf{w}, \phi_h) - B(\tilde{\mathbf{w}}, \mathbf{w}, \phi_h)| + |B(\tilde{\mathbf{w}}, \mathbf{w}, \phi_h) - B(\tilde{\mathbf{w}}, \tilde{\mathbf{w}}, \phi_h)| \\
& \leq M_a \mu \delta^{\sigma+1} (\|\nabla \boldsymbol{\eta}\|_F \|\nabla \mathbf{w}\|_F, \|\nabla \phi_h\|_F) \\
& + M_a \mu \delta^{\sigma+1} (\|\nabla \tilde{\mathbf{w}}\|_F \|\nabla \boldsymbol{\eta}\|_F, \|\nabla \phi_h\|_F). \tag{5.10}
\end{aligned}$$

Note that the stability estimates in [12] imply

$$\|\nabla \tilde{\mathbf{w}}\|_{\mathbf{L}^\infty} \leq \tilde{C} \|\nabla \mathbf{w}\|_{\mathbf{L}^\infty}. \tag{5.11}$$

Thus,

$$\begin{aligned}
& B(\mathbf{w}, \mathbf{w}, \phi_h) - B(\tilde{\mathbf{w}}, \tilde{\mathbf{w}}, \phi_h) \\
& \leq M_a \mu \delta^{\sigma+1} \|\nabla \mathbf{w}\|_{\mathbf{L}^\infty} \|\nabla \boldsymbol{\eta}\| \|\nabla \phi_h\| + M_a \mu \delta^{\sigma+1} \tilde{C} \|\nabla \mathbf{w}\|_{\mathbf{L}^\infty} \|\nabla \boldsymbol{\eta}\| \|\nabla \phi_h\| \\
& \leq C(M_a, \mu, \delta, \sigma, \tilde{C}) \frac{1}{4\varepsilon_2} \|\nabla \mathbf{w}\|_{\mathbf{L}^\infty}^2 \|\nabla \boldsymbol{\eta}\|^2 + \varepsilon_2 \|\nabla \phi_h\|^2. \tag{5.12}
\end{aligned}$$

By adding and subtracting terms, we obtain

$$\begin{aligned}
& C(\mathbf{w}, \mathbf{w}, \phi_h) - C(\mathbf{w}_h, \mathbf{w}_h, \phi_h) \\
& \leq |C(\mathbf{w}, \mathbf{w}, \phi_h) - C(\mathbf{w}_h, \mathbf{w}, \phi_h)| + |C(\mathbf{w}_h, \mathbf{w}, \phi_h) - C(\mathbf{w}_h, \mathbf{w}_h, \phi_h)| \\
& = |((\boldsymbol{\eta} + \phi_h) \cdot \nabla \mathbf{w}, \phi_h)| + |(\mathbf{w}_h \cdot \nabla(\boldsymbol{\eta} + \phi_h), \phi_h)| \\
& \leq |(\boldsymbol{\eta} \cdot \nabla \mathbf{w}, \phi_h)| + |(\phi_h \cdot \nabla \mathbf{w}, \phi_h)| + |(\mathbf{w}_h \cdot \nabla \boldsymbol{\eta}, \phi_h)| + |(\mathbf{w}_h \cdot \nabla \phi_h, \phi_h)| \\
& \leq \left(\frac{1}{2} \|\boldsymbol{\eta}\|^2 + \frac{1}{2} \|\nabla \mathbf{w}\|_{\mathbf{L}^\infty}^2 \|\phi_h\|^2 \right) + (\|\nabla \mathbf{w}\|_{\mathbf{L}^\infty}^2 \|\phi_h\|^2) \\
& + \left(\frac{1}{2} \|\nabla \boldsymbol{\eta}\|^2 + \frac{1}{2} \|\nabla \mathbf{w}\|_{\mathbf{L}^\infty}^2 \|\phi_h\|^2 \right) + \left(\varepsilon_3 \|\nabla \phi_h\|^2 + \frac{1}{4\varepsilon_3} \|\mathbf{w}_h\|_{\mathbf{L}^\infty}^2 \|\phi_h\|^2 \right) \tag{5.13}
\end{aligned}$$

By using the Cauchy-Schwartz and Young's inequalities, we obtain

$$(q - \lambda_h, \nabla \cdot \phi_h) \leq |(q - \lambda_h, \nabla \cdot \phi_h)| \leq \varepsilon_4 \|\nabla \phi_h\|^2 + \frac{1}{4\varepsilon_4} \|q - \lambda_h\|^2. \tag{5.14}$$

Inserting estimates (5.7)-(5.14) into (5.6), and picking $\varepsilon_1 := 1/8$, $\varepsilon_2 := Re^{-1}/8$, $\varepsilon_3 := Re^{-1}/8$, $\varepsilon_4 := Re^{-1}/8$, we get

$$\begin{aligned}
& \frac{1}{2} \frac{d}{dt} \|\phi_h\|^2 + \frac{Re^{-1}}{2} \|\nabla \phi_h\|^2 \\
& \leq \left(\frac{1}{2} + 2Re^{-1} + 2Re C(M_a, \mu, \delta, \sigma, \tilde{C}) \|\nabla \mathbf{w}\|_{\mathbf{L}^\infty}^2 \right) \|\nabla \boldsymbol{\eta}\|^2 \\
& + \frac{1}{2} \|\boldsymbol{\eta}_t\|^2 + \frac{1}{2} \|\boldsymbol{\eta}\|^2 + 2Re \|q - \lambda_h\|^2 \\
& + \left(\frac{1}{2} + \frac{1}{2} \|\nabla \mathbf{w}\|_{\mathbf{L}^\infty}^2 + \|\nabla \mathbf{w}\|_{\mathbf{L}^\infty} + \frac{1}{2} \|\mathbf{w}\|_{\mathbf{L}^\infty}^2 + 2Re \|\mathbf{w}_h\|_{\mathbf{L}^\infty}^2 \right). \tag{5.15}
\end{aligned}$$

In order to apply Gronwall's lemma, we need

$$\begin{aligned}
b(t) & := \left(\frac{1}{2} + \frac{1}{2} \|\nabla \mathbf{w}\|_{\mathbf{L}^\infty}^2 + \|\nabla \mathbf{w}\|_{\mathbf{L}^\infty} + \frac{1}{2} \|\mathbf{w}\|_{\mathbf{L}^\infty}^2 + 2Re \|\mathbf{w}_h\|_{\mathbf{L}^\infty}^2 \right) \\
& \in L^1(0, T). \tag{5.16}
\end{aligned}$$

This follows immediately from the hypothesis ($\mathbf{w} \in L^4(0, T; \mathbf{W}^{1,\infty}(\Omega))$) and the stability estimate for \mathbf{w}_h (Lemma 4.6).

Hiding all constants in generic C 's, Gronwall's lemma now implies, for almost all $t \in [0, T]$, that

$$\begin{aligned}
& \|\phi_h(\mathbf{x}, t)\|^2 + Re^{-1} \|\nabla \phi_h\|_{L^2(0,t;L^2)}^2 \\
& \leq C \exp(\|b(t)\|_{L^1(0,t)}) \|\phi_h(\mathbf{x}, 0)\|^2 \\
& + C \exp(\|b(t)\|_{L^1(0,t)}) \left[\frac{1}{2} \|\eta_t\|_{L^2(0,t;L^2)}^2 + \frac{1}{2} \|\eta\|_{L^2(0,t;L^2)}^2 \right. \\
& + \left. \left(\frac{1}{2} + 2Re^{-1} \right) \frac{1}{2} \|\nabla \eta\|_{L^2(0,t;L^2)}^2 + C(\delta, \mathbf{w}, a) \int_0^t 2Re \|\nabla \mathbf{w}\|_{L^\infty}^2 \|\nabla \eta\|^2 ds \right. \\
& \left. + 2Re \|q - \lambda_h\|^2 \right]. \tag{5.17}
\end{aligned}$$

By using the Cauchy-Schwartz inequality in $L^2(0, t)$, $t \in [0, T]$, and the hypothesis ($\mathbf{w} \in L^4(0, T; \mathbf{W}^{1,\infty}(\Omega))$), we get

$$\int_0^t \|\nabla \mathbf{w}\|_{L^\infty}^2 \|\nabla \eta\|^2 ds \leq \|\nabla \mathbf{w}\|_{L^4(0,t;L^\infty)}^2 \|\nabla \eta\|_{L^4(0,t;L^2)}^2. \tag{5.18}$$

We apply now the essential supremum over $t \in [0, T]$ on both sides of inequality (5.17). By using the triangle inequality, the error estimate in the theorem now follows. ■

REMARK 5.1. *The error estimate in Theorem 5.1 is not uniform in Re , as the error estimate for the Smagorinsky model (Theorem 4.2 in [31]). The reason is that our bounded AV operator $B(\cdot, \cdot, \cdot)$ is just monotone (Lemma 4.1), and not strongly monotone as the Smagorinsky AV operator in [31].*

REMARK 5.2. *The regularity of \mathbf{w} ($\mathbf{w} \in L^4(0, T; \mathbf{W}^{1,\infty}(\Omega))$) assumed in Theorem 5.1 is higher than the regularity of \mathbf{w} assumed in the error estimate for the Smagorinsky model in [31] ($\mathbf{w} \in L^2(0, T; \mathbf{W}^{1,\infty}(\Omega))$). Again, the reason is that our bounded AV operator $B(\cdot, \cdot, \cdot)$ is just monotone (Lemma 4.1), whereas the Smagorinsky AV operator is strongly monotone.*

REMARK 5.3. *The multiplicative constant $C_1(\mathbf{w}, Re) := \exp(\|b(t)\|_{L^1(0,T)})$ in the error estimate in Theorem 5.1 depends on Re . Note, however, that if we use the skew-symmetric form of $C(\cdot, \cdot, \cdot)$, i.e.*

$$C_{skew-symmetric}(\mathbf{u}, \mathbf{v}, \mathbf{w}) := \frac{1}{2} C(\mathbf{u}, \mathbf{v}, \mathbf{w}) - \frac{1}{2} C(\mathbf{u}, \mathbf{w}, \mathbf{v}), \tag{5.19}$$

the last term in the last inequality in (5.13) disappears, and thus the corresponding term $2Re \|\mathbf{w}_h\|_{L^\infty}^2$ multiplying $\|\phi_h\|^2$ in (5.15) disappears as well. Therefore, $b(t)$ in (5.16) becomes independent of Re .

COROLLARY 5.2. *The order of convergence of*

$$\|\mathbf{w} - \mathbf{w}_h\|_{L^\infty(0,T;L^2)} \text{ is } O(h^{k+1}), \tag{5.20}$$

$$\|\mathbf{w} - \mathbf{w}_h\|_{L^2(0,T;L^2)} \text{ is } O(h^{k+1}), \tag{5.21}$$

$$\|\mathbf{w} - \mathbf{w}_h\|_{L^2(0,T;H^1)} \text{ is } O(h^k). \tag{5.22}$$

Proof. The proof is an immediate consequence of Theorem 5.1 and the approximation properties of the interpolation (3.7)–(3.9). ■

6. Newton Approximation Scheme for the Bounded AV Model. In this section, we discuss the Newton approximation scheme as applied to the Navier-Stokes equations with the bounded artificial viscosity term (1.2). The analysis in this section is especially relevant to the numerical discretization of the vortex decay problem used in Section 7.2.1. Note that approximate solutions $(\mathbf{u}_h, p_h) \in \mathbf{X}_h \times Q_h$ must satisfy a nonlinear system of ordinary differential equations. In this section, we derive the Newton approximation scheme for the semi-discrete variational problem, and note that, in practice, one would apply a Newton iteration at each time step for a fully discrete approximation.

We first derive the Gâteaux derivative for the bounded artificial viscosity term considered in this paper.

THEOREM 6.1. *Suppose that the function $a(\cdot) : \mathbb{R} \rightarrow \mathbb{R}$ is analytic, and define the (continuous) map $\mathcal{G}_1 : \mathbf{X}_h \rightarrow \mathbf{X}_h$ as*

$$\langle \mathcal{G}_1[\mathbf{u}], \mathbf{v} \rangle := (a(\|\nabla \mathbf{u}\|_F) \nabla \mathbf{u}, \nabla \mathbf{v}).$$

Then the Gâteaux derivative in the direction of \mathbf{u} evaluated at \mathbf{w} , denoted as $\mathcal{J}_u \mathcal{G}_1[\mathbf{w}]$, is equal to

$$\langle \mathcal{J}_u \mathcal{G}_1[\mathbf{w}], \mathbf{v} \rangle = (a(\|\nabla \mathbf{u}\|_F) \nabla \mathbf{w}, \nabla \mathbf{v}) + \left(\frac{a'(\|\nabla \mathbf{u}\|_F)}{\|\nabla \mathbf{u}\|_F} [\nabla \mathbf{u} : \nabla \mathbf{w}] \nabla \mathbf{u}, \nabla \mathbf{v} \right)$$

Proof. Under the assumption that $a(\cdot)$ is analytic, we have a Taylor series expansion

$$a(x) = \sum_{n=0}^{\infty} \frac{a^{(n)}(0) x^n}{n!}.$$

Therefore,

$$\langle \mathcal{G}_1[\mathbf{u}], \mathbf{v} \rangle = \sum_{n=0}^{\infty} \frac{a^{(n)}(0)}{n!} (\|\nabla \mathbf{u}\|_F^n \nabla \mathbf{u}, \nabla \mathbf{v}).$$

For $n = 0$, it is clear that

$$\langle \mathcal{J}_u \nabla \mathbf{w}, \nabla \mathbf{v} \rangle = (\nabla \mathbf{w}, \nabla \mathbf{v}),$$

and we have the formula for generic $n \geq 1$,

$$\langle \mathcal{J}_u \|\nabla \mathbf{w}\|_F^n \nabla \mathbf{w}, \nabla \mathbf{v} \rangle = (\|\nabla \mathbf{u}\|_F^n \nabla \mathbf{w}, \nabla \mathbf{v}) + n (\|\nabla \mathbf{u}\|_F^{n-2} [\nabla \mathbf{u} : \nabla \mathbf{w}] \nabla \mathbf{u}, \nabla \mathbf{v}).$$

Therefore, we have that

$$\begin{aligned} & \langle \mathcal{J}_u \mathcal{G}_1[\mathbf{w}], \mathbf{v} \rangle \\ &= \sum_{n=0}^{\infty} \frac{a^{(n)}(0)}{n!} (\|\nabla \mathbf{u}\|_F^n \nabla \mathbf{w}, \nabla \mathbf{v}) + \sum_{n=1}^{\infty} \frac{n a^{(n)}(0)}{n!} (\|\nabla \mathbf{u}\|_F^{n-2} [\nabla \mathbf{u} : \nabla \mathbf{w}] \nabla \mathbf{u}, \nabla \mathbf{v}) \\ &= \sum_{n=0}^{\infty} \frac{a^{(n)}(0)}{n!} (\|\nabla \mathbf{u}\|_F^n \nabla \mathbf{w}, \nabla \mathbf{v}) + \sum_{n=1}^{\infty} \frac{a^{(n)}(0)}{(n-1)!} \left(\frac{\|\nabla \mathbf{u}\|_F^{n-1}}{\|\nabla \mathbf{u}\|_F} [\nabla \mathbf{u} : \nabla \mathbf{w}] \nabla \mathbf{u}, \nabla \mathbf{v} \right) \\ &= (a(\|\nabla \mathbf{u}\|_F) \nabla \mathbf{w}, \nabla \mathbf{v}) + \left(\frac{a'(\|\nabla \mathbf{u}\|_F)}{\|\nabla \mathbf{u}\|_F} [\nabla \mathbf{u} : \nabla \mathbf{w}] \nabla \mathbf{u}, \nabla \mathbf{v} \right) \end{aligned}$$

COROLLARY 6.2. *Suppose that the function $a(\cdot) : \mathbb{R} \rightarrow \mathbb{R}$ is analytic, and define the (continuous) map $\mathcal{G}_2 : \mathbf{X}_h \rightarrow \mathbf{X}_h$ as*

$$\langle \mathcal{G}_2[\mathbf{u}], \mathbf{v} \rangle := (a(\delta \|\nabla \mathbf{u}\|_F) \nabla \mathbf{u}, \nabla \mathbf{v}).$$

Then the Gâteaux derivative in the direction of \mathbf{u} evaluated at \mathbf{w} , denoted as $\mathcal{J}_{\mathbf{u}} \mathcal{G}_2[\mathbf{w}]$ is equal to

$$\langle \mathcal{J}_{\mathbf{u}} \mathcal{G}_2[\mathbf{w}], \mathbf{v} \rangle = (a(\delta \|\nabla \mathbf{w}\|_F) \nabla \mathbf{w}, \nabla \mathbf{v}) + \delta \left(\frac{a'(\delta \|\nabla \mathbf{u}\|_F)}{\|\nabla \mathbf{u}\|_F} [\nabla \mathbf{u} : \nabla \mathbf{w}] \nabla \mathbf{u}, \nabla \mathbf{v} \right)$$

We now consider the semi-discrete approximation $(\mathbf{u}_h, p_h) \in \mathbf{X}_h \times Q_h$ which solves the overall Navier-Stokes system with bounded artificial viscosity term (1.2). For notational simplicity, we drop the “ h ” subscripts from \mathbf{u} and p . Define the (continuous) map $\mathcal{G} : \mathbf{X}_h \times Q_h \rightarrow \mathbf{X}_h \times Q_h$ as

$$\begin{aligned} \langle \mathcal{G}[\mathbf{u}, p], (\mathbf{v}, q) \rangle &:= (\mathbf{u}_t, \mathbf{v}) + Re^{-1} (\nabla \mathbf{u}, \nabla \mathbf{v}) + \mu \delta^\sigma (a(\delta \|\nabla \mathbf{u}\|_F) \nabla \mathbf{u}, \nabla \mathbf{v}) \\ &\quad + (\mathbf{u} \cdot \nabla \mathbf{u}, \mathbf{v}) - (p, \nabla \cdot \mathbf{v}) + (q, \nabla \cdot \mathbf{u}) - (\mathbf{f}, \mathbf{v}). \end{aligned}$$

Therefore, we immediately have that the Gâteaux derivative of \mathcal{G} in the direction of (\mathbf{u}, p) , evaluated at (\mathbf{w}, r) is given by

$$\begin{aligned} \langle \mathcal{J}_{(\mathbf{u}, p)} \mathcal{G}[\mathbf{w}, r], (\mathbf{v}, q) \rangle &= (\mathbf{w}_t, \mathbf{v}) + Re^{-1} (\nabla \mathbf{w}, \nabla \mathbf{v}) + \mu \delta^\sigma (a(\delta \|\nabla \mathbf{u}\|_F) \nabla \mathbf{w}, \nabla \mathbf{v}) \\ &\quad + \mu \delta^{\sigma+1} \left(\frac{a'(\delta \|\nabla \mathbf{u}\|_F)}{\|\nabla \mathbf{u}\|_F} [\nabla \mathbf{u} : \nabla \mathbf{w}] \nabla \mathbf{u}, \nabla \mathbf{v} \right) \\ &\quad + (\mathbf{u} \cdot \nabla \mathbf{w}, \mathbf{v}) + (\mathbf{w} \cdot \nabla \mathbf{u}, \mathbf{v}) \\ &\quad - (r, \nabla \cdot \mathbf{v}) + (q, \nabla \cdot \mathbf{w}) - (\mathbf{f}, \mathbf{v}) \end{aligned}$$

Now, substituting this formula for $\langle \mathcal{J}_{(\mathbf{u}, p)} \mathcal{G}[\mathbf{w}, r], (\mathbf{v}, q) \rangle$ into the Newton iteration system

$$\left\langle \mathcal{J}_{(\mathbf{u}^{(n-1)}, p^{(n-1)})} \mathcal{G}[\mathbf{u}^{(n)} - \mathbf{u}^{(n-1)}, p^{(n)} - p^{(n-1)}], (\mathbf{v}, q) \right\rangle = - \left\langle \mathcal{G}[\mathbf{u}^{(n-1)}, p^{(n-1)}], (\mathbf{v}, q) \right\rangle,$$

we obtain the Newton iteration scheme

$$\begin{aligned} &(\mathbf{u}_t^{(n)}, \mathbf{v}) + Re^{-1} (\nabla \mathbf{u}^{(n)}, \nabla \mathbf{v}) + \mu \delta^\sigma (a(\delta \|\nabla \mathbf{u}^{(n-1)}\|_F) \nabla \mathbf{u}^{(n)}, \nabla \mathbf{v}) \\ &+ \mu \delta^{\sigma+1} \left(\frac{a'(\delta \|\nabla \mathbf{u}^{(n-1)}\|_F)}{\|\nabla \mathbf{u}^{(n-1)}\|_F} [\nabla \mathbf{u}^{(n-1)} : \nabla \mathbf{u}^{(n)}] \nabla \mathbf{u}^{(n-1)}, \nabla \mathbf{v} \right) \\ &+ (\mathbf{u}^{(n-1)} \cdot \nabla \mathbf{u}^{(n)}, \mathbf{v}) + (\mathbf{u}^{(n)} \cdot \nabla \mathbf{u}^{(n-1)}, \mathbf{v}) - (p^{(n)}, \nabla \cdot \mathbf{v}) + (q, \nabla \cdot \mathbf{u}^{(n)}) \\ &= (\mathbf{f}, \mathbf{v}) + \mu \delta^{\sigma+1} (a'(\delta \|\nabla \mathbf{u}^{(n-1)}\|_F) \|\nabla \mathbf{u}^{(n-1)}\|_F \nabla \mathbf{u}^{(n-1)}, \nabla \mathbf{v}) + (\mathbf{u}^{(n-1)} \cdot \nabla \mathbf{u}^{(n-1)}, \mathbf{v}) \end{aligned} \tag{6.1}$$

for all $(\mathbf{v}, q) \in \mathbf{X}_h \times Q_h$.

REMARK 6.1. *Given an initial $(\mathbf{u}^{(0)}, p^{(0)}) \in \mathbf{X}_h \times Q_h$, the existence of a solution $(\mathbf{u}^{(n)}, p^{(n)}) \in \mathbf{X}_h \times Q_h$ for all $n = 1, 2, \dots$ to (6.1) follows by using the same arguments as in Section 4 (Lemmas 4.6 and 4.7). Since the system (6.1), however, is linear, we can easily prove (by using the properties of $a(\cdot)$) that the solution $(\mathbf{u}^{(n)}, p^{(n)})$ is also unique.*

7. Numerical Results. In this section we present numerical results for the bounded AV model (2.12)–(2.14). We start by illustrating the improvement in the bounded AV model over the overly dissipative Smagorinsky model in the numerical simulation of a 3D channel flow (Section 7.1). We then present a careful mesh refinement study supporting the error estimates (Section 7.2).

7.1. Improvement in the BAV Model. In this section, we illustrate the improvement in the bounded AV model over the Smagorinsky model when applied to a 3D channel flow.

We chose the computational domain $\Omega = (-0.5, 0.5) \times (-0.5, 0.5) \times (0, 10) \subset \mathbf{R}^3$, Dirichlet boundary conditions at the inlet ($z = 0$), on top ($x = 0.5$) and bottom ($x = -0.5$), and “do-nothing” boundary conditions (i.e., $(-p\mathbb{I} + 2Re^{-1}\nabla^s\mathbf{u}) \cdot \mathbf{n} = 0$) at the outlet ($z = 10$). The boundary conditions and the forcing term have been chosen so that the system (u, v, w, p) defined by

$$\begin{aligned} u(x, y, z) &= 0, \\ v(x, y, z) &= 0, \\ w(x, y, z) &= 1600(x^2 - 0.25)(y^2 - 0.25), \\ p(x, y, z) &= 3200Re^{-1}(x^2 + y^2 - 0.5), \end{aligned}$$

satisfy the stationary Navier-Stokes system. This choice results in homogeneous boundary conditions on top and bottom, parabolic inflow profile, and identically zero forcing term. We used the exact solution as initial condition.

We chose a large value for the horizontal velocity ($w = 100$) in the center of the channel ($x = y = 0.0$) since we wanted to compare the Smagorinsky model and the bounded AV model in flows displaying two regimes: (a) moderate/low velocity deformation tensors; and (b) high velocity deformation tensors. Our choice displays both regimes: the center of the channel displays regime (a) ($\|\nabla^s\mathbf{u}\|_F = 0$) and the near-wall region displays regime (b) ($\|\nabla^s\mathbf{u}\|_F = 200\sqrt{2}$).

We also chose $Re = 10^3$.

The numerical simulations in this section have been carried out with the Virginia Tech Large Eddy Simulator (ViTLES) (see Appendix A for a detailed description of the algorithm and computational implementation). We used a coarse nonuniform mesh of size $h = 0.5$, a small time-step $\Delta t = 10^{-3}$, and a small penalty parameter $\varepsilon = 10^{-4}$ in the penalty method to compute the pressure.

Since we use Taylor-Hood finite element spaces for the spatial discretization and Crank-Nicolson for the time-discretization, we expect that the leading term in the total error will be given by the spatial discretization for these small choices for Δt and ε ($O(h^2) \gg O(\Delta t^2) + O(\varepsilon)$). The nonlinear system at each time-step is solved with a Newton iteration up to an Euclidian norm of the residual vector less than 10^{-8} . The final time is $T = 0.1$ (i.e., 10^2 time-steps). Since $w = 100$ in the center of the channel, this allows a particle in the center to travel the entire length of the channel once.

It is clear that, since we have an exact solution, this flow is *not* turbulent. We chose this setting, however, because in the next section we will investigate the behavior of the error with respect to the mesh refinement (and thus we need the exact solution). Obviously, a real turbulent flow numerical comparison of the Smagorinsky and the bounded AV models is needed and will be carried out in a future study.

Figures 7.1–7.2 present numerical results for: (i) the exact solution; (ii) a coarse, under-resolved numerical simulation (just the NSE, without any SGS model); (iii) the

Smagorinsky model (1.1); and (iv) the bounded AV model (1.2).

We chose a filter radius $\delta = 0.5$. This relatively large value for δ increased the effect of the SGS models on the numerical results, allowing a clearer comparison. We also chose the Smagorinsky constant $c_s = 0.17$, which is a popular choice in the literature. For the bounded AV model, we chose $\mu \sim 0.4$ and $\sigma = 1$. These parameter choices for the bounded AV model are not optimal, and further testing is needed to find the optimal values. The function $a(\cdot)$ was chosen to resemble that in Figure 1:

$$a(\delta \|\nabla^s \mathbf{u}\|_F) := -0.02 + \frac{1}{1 + 49 e^{-5.7\delta \|\nabla^s \mathbf{u}\|_F}} \quad (7.1)$$

This is exactly the function that was chosen in [27] for a *completely different setting* (a rotating pulse for the convection-diffusion equation). Thus, this choice is most probably not optimal for our present setting. We emphasize that we compare the Smagorinsky model with tuned parameters with the bounded AV model with non-optimized parameters.

Figure 7.1 presents the horizontal velocity component (w) for the exact solution, an under-resolved (no SGS model) numerical simulation, the Smagorinsky model, and the bounded AV model. It is clear that the under-resolved simulation yields completely inaccurate results. This illustrates the need for SGS modeling at this mesh resolution and Reynolds number. The Smagorinsky model yields improved results. The horizontal velocity in the center of the channel, however, is too high (107 instead of 100). The bounded AV model yields the best results.

But the most dramatic results are those for the pressure (p) in Figure 7.2. The under-resolved simulation yields again very inaccurate results. The Smagorinsky model yields again better results, but this time the pressure gradient is **10 times higher** than that for the bounded AV model.

This behavior is the perfect illustration of the improvement of the bounded AV model over the Smagorinsky model. Indeed, the Smagorinsky model is overly diffusive and introduces an unphysical amount of AV. Thus, the pressure gradient needs to increase dramatically to keep the same flow rate through the channel. The bounded AV model, on the other hand, introduces a moderate amount of AV which requires a much more realistic pressure gradient.

7.2. Mesh Refinement Study. In this section, we present a careful mesh refinement study supporting the error estimates in Theorem 5.1 for the bounded AV model (1.2).

7.2.1. The 2D Vortex Decay Problem. In this section, we present numerical results for the bounded AV model applied to the vortex decay problem of Chorin [9, 51]. A similar study for the vortex decay problem using the Smagorinsky model was presented in [31]. For the vortex decay problem, we define the domain $\Omega = (0, 1)^2 \subset \mathbf{R}^2$, and specify

$$\begin{aligned} u_1 &:= -\cos(n\pi x) \sin(n\pi y) \exp(-2n^2\pi^2 t/\tau), \\ u_2 &:= \sin(n\pi x) \cos(n\pi y) \exp(-2n^2\pi^2 t/\tau), \\ p &:= -\frac{1}{4}(\cos(2n\pi x) + \cos(2n\pi y)) \exp(-4n^2\pi^2 t/\tau). \end{aligned} \quad (7.2)$$

Note that for $\tau := \text{Re}^{-1}$, the set (u_1, u_2, p) solves the time-dependent Navier-Stokes equations with the appropriate (time dependent, Dirichlet) boundary conditions. For our purposes, we take (7.2) as the solution to (2.12)–(2.14) and illustrate two points:

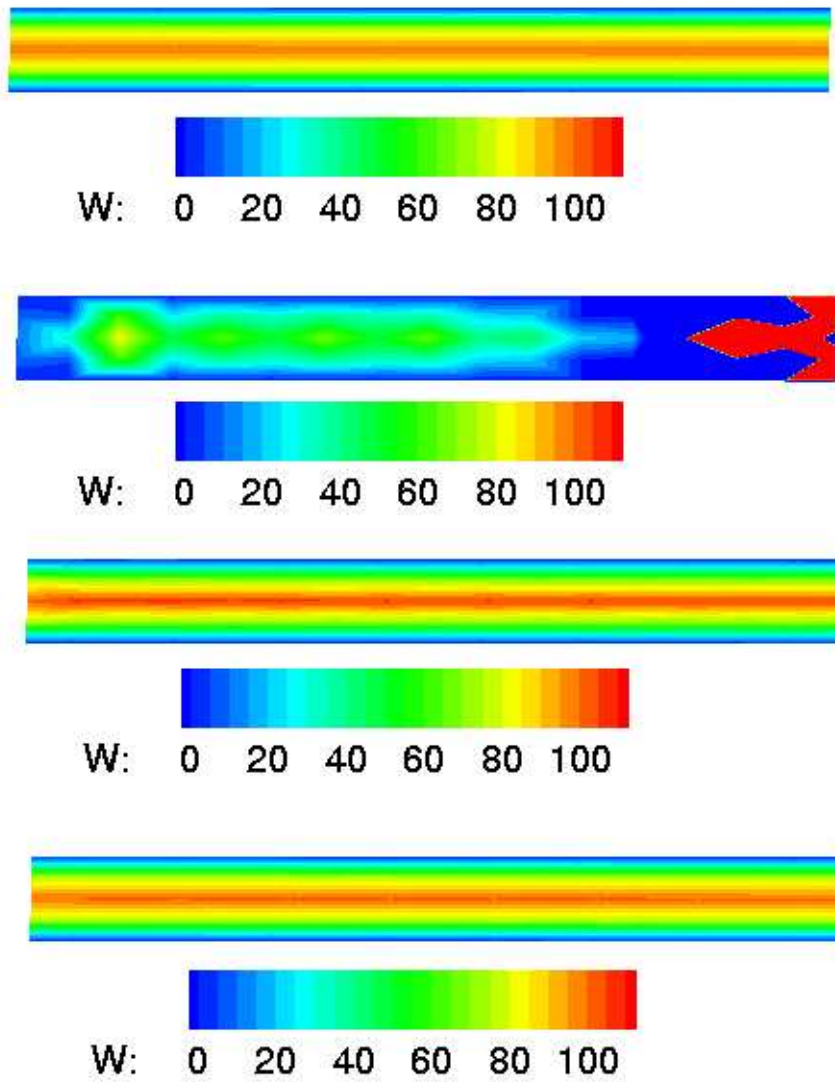


FIG. 7.1. 3D channel flow, coarse mesh, vertical cross section. The horizontal velocity distribution (top to bottom): Exact solution (first); Navier-Stokes (second); Smagorinsky (third); and BAV (fourth).

that the spatial semi-discretization error estimates (5.20)–(5.22) in Corollary 5.2 are satisfied and that the estimates are bounded uniformly with respect to the Reynolds number.

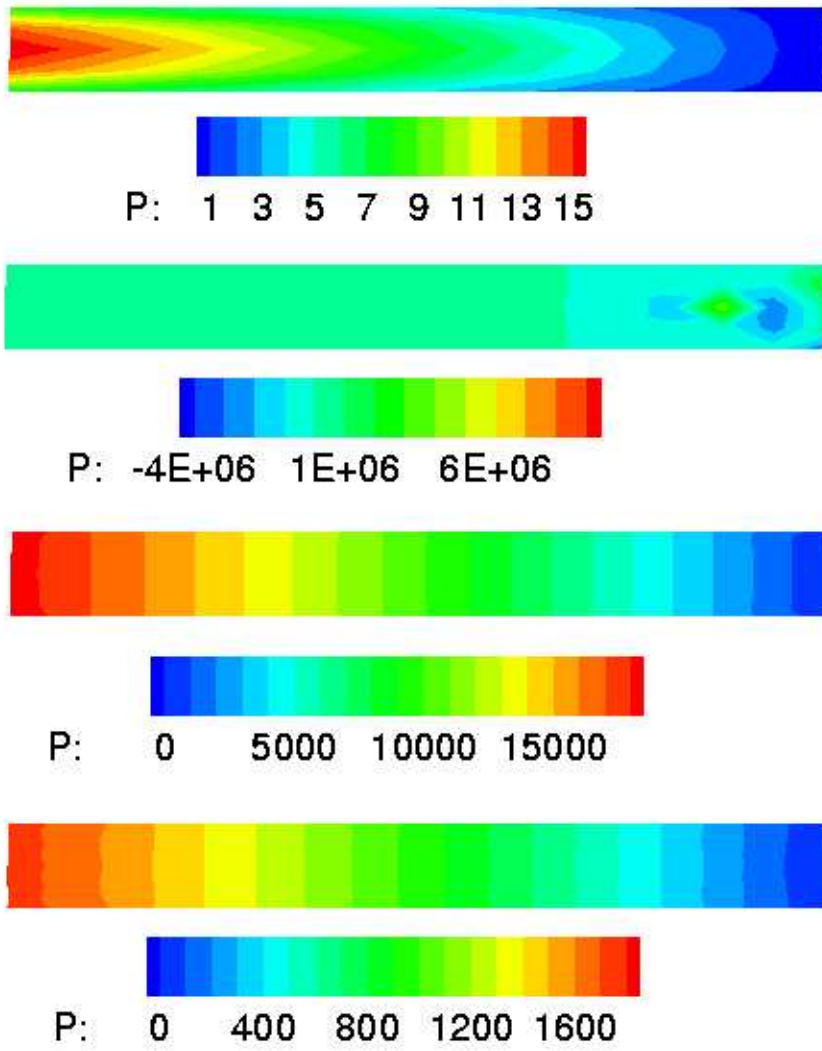


FIG. 7.2. 3D channel flow, coarse mesh, vertical cross section. The pressure distribution (top to bottom): Exact solution (first); Navier-Stokes (second); Smagorinsky (third); and BAV (fourth).

Accordingly, we specify the following parameters,

$$\begin{aligned}
 \text{Re} &:= 10^{10}, \\
 \tau &:= 1000, \\
 \text{final time } T &:= 2, \\
 \text{filter radius } \delta &:= 0.1, \\
 \mu = c_s^2 &:= 0.17^2, \\
 \Delta t &:= 0.01.
 \end{aligned}$$

For our calculations, we assume $n = 3$, i.e. a 3×3 array of vortices and study

h	$\ \mathbf{w} - \mathbf{w}_h\ _{L^\infty(0,T;L^2)}$	rate	$\ \mathbf{w} - \mathbf{w}_h\ _{L^2(0,T;L^2)}$	rate	$\ \mathbf{w} - \mathbf{w}_h\ _{L^2(0,T;H^1)}$	rate
1/8	$4.020927 \cdot 10^{-1}$		$4.936365 \cdot 10^{-1}$		$1.560773 \cdot 10^1$	
1/16	$3.103567 \cdot 10^{-2}$	3.70	$3.952673 \cdot 10^{-2}$	3.64	$2.886625 \cdot 10^0$	2.43
1/24	$5.534371 \cdot 10^{-3}$	4.25	$7.594030 \cdot 10^{-3}$	4.07	$1.096755 \cdot 10^0$	2.39
1/32	$1.822532 \cdot 10^{-3}$	3.86	$2.418206 \cdot 10^{-3}$	3.98	$5.182457 \cdot 10^{-1}$	2.61
1/40	$7.778230 \cdot 10^{-4}$	3.82	$1.018835 \cdot 10^{-3}$	3.87	$2.870239 \cdot 10^{-1}$	2.65
1/48	$4.227375 \cdot 10^{-4}$	3.34	$5.138958 \cdot 10^{-4}$	3.75	$1.763596 \cdot 10^{-1}$	2.68
1/56	$2.567581 \cdot 10^{-4}$	3.26	$2.907396 \cdot 10^{-4}$	3.70	$1.166515 \cdot 10^{-1}$	2.68
1/64	$1.645877 \cdot 10^{-4}$	3.33	$1.779283 \cdot 10^{-4}$	3.68	$8.151033 \cdot 10^{-2}$	2.68
1/72	$1.102856 \cdot 10^{-4}$	3.40	$1.154125 \cdot 10^{-4}$	3.68	$5.940966 \cdot 10^{-2}$	2.69

TABLE 7.1

Finite element convergence estimates for the vortex decay problem.

the finite element convergence rates for fixed $\delta := 0.1$ as $h \rightarrow 0$. For the spatial discretization, we take the Taylor-Hood finite element pair and implement the Newton iteration scheme as described in Section 6. For the temporal discretization, we use the Crank-Nicolson scheme. Indicated in Table 7.1, the spatial semi-discretization convergence estimates follow their predicted values of 3 in the spatial L^2 norm and 2 in the spatial H^1 norm. Also, note that these estimates are *independent* of the selected Reynolds number, as we have taken a relatively high value for Re and a relatively high value for Δt .

Appendix A. The Virginia Tech Large Eddy Simulator (ViTLES).

In this paper, we have used *ViTLES*, the Virginia Tech Large Eddy Simulator, a *parallel, finite element* computational platform for the numerical validation of CFD and LES models. In the sequel, we describe algorithms central to efficient, reliable computational simulations.

A.1. Algorithm: Spatial Discretization. For spatial discretization, the computational domain is decomposed in a collection of non-overlapping triangles (in 2D) or tetrahedra (in 3D). Thus, the geometric flexibility of FE allows us to treat complex geometries. We employ the traditional Taylor-Hood finite element pair (continuous quadratic velocities and continuous linear pressures) which satisfies the discrete inf-sup (LBB_h) condition [8].

A.2. Algorithm: Time Discretization. For time discretization, we employ the second-order accurate, unconditionally stable Crank-Nicolson scheme [13]. Thus, for each time step, we solve the following nonlinear system of equations:

$$\begin{aligned} & \frac{\mathbf{u}^{k+1} - \mathbf{u}^k}{\Delta t} - \theta \nabla \cdot (2Re^{-1} \nabla^s \mathbf{u}^{k+1}) + \theta (\mathbf{u}^{k+1} \cdot \nabla) \mathbf{u}^{k+1} + \theta \nabla p^{k+1} \\ & = (1 - \theta) \nabla \cdot (2Re^{-1} \nabla^s \mathbf{u}^k) - (1 - \theta) (\mathbf{u}^k \cdot \nabla) \mathbf{u}^k - (1 - \theta) \nabla p^k + \theta \mathbf{f}^{k+1} + (1 - \theta) \mathbf{f}^k, \end{aligned} \quad (\text{A.1})$$

where $(\mathbf{u}^{k+1}, p^{k+1}, \mathbf{f}^{k+1})$ and $(\mathbf{u}^k, p^k, \mathbf{f}^k)$ are the velocity, pressure, and forcing vectors at the current and previous time-step, respectively, $\theta = \frac{1}{2}$ for Crank-Nicolson, and Δt is the time-step.

A.3. Algorithm: Penalty Method. Another popular approach to increasing the computational speed in CFD flow simulations is the penalty method [13, 25, 44].

The incompressibility constraint $\nabla \cdot \mathbf{u} = 0$ in the Navier-Stokes equations (2.1)–(2.3) is relaxed by setting

$$\varepsilon p_\varepsilon + \nabla \cdot \mathbf{u}_\varepsilon = 0, \quad (\text{A.2})$$

where ε is a small parameter. Obviously, the incompressibility constraint is no longer satisfied, but it can be proven that (e.g. formula (5.16) in [25])

$$\|\mathbf{u} - \mathbf{u}_\varepsilon\|_1 + \|p - p_\varepsilon\|_0 \leq C \varepsilon.$$

Thus, as $\varepsilon \rightarrow 0$, the solution of the penalized problem converges to that of the unpenalized problem. In our computations, we used $\varepsilon = 0.0001$. The time discretization we chose for the penalty method reads

$$\varepsilon p^{k+1} + \nabla \cdot \mathbf{u}^{k+1} = \varepsilon p^k,$$

where the $k + 1$ superscript denotes the current time step, and the k superscript denotes the previous time step. In this form, the penalty method resembles the artificial compressibility method [25, 13], the augmented lagrangian method [44], or the iterated penalty method [25].

A.4. Algorithm: Newton Iteration. In this section we describe a Newton iteration scheme for solving the nonlinear system at each time step. The scheme implemented in ViTLES explicitly constructs approximations of the Jacobians rather than calculating the actual Jacobian matrix. Such a scheme provides rapid computational implementation, and is easily transportable in the sense of applicability to a number of physical problems.

In view of (A.1) and (A.2), at each time-step we solve

$$R(\mathbf{u}^{k+1}, p^{k+1}) = \mathbf{0}$$

where

$$\begin{aligned} & R(\mathbf{u}^{k+1}, p^{k+1}) \\ & := (\mathbf{u}^{k+1} - \theta \Delta t \nabla \cdot (2Re^{-1} \nabla^s \mathbf{u}^{k+1}) + \theta \Delta t (\mathbf{u}^{k+1} \cdot \nabla) \mathbf{u}^{k+1} + \theta \Delta t \nabla p^{k+1} + R_k, \\ & \quad \nabla \cdot \mathbf{u}^{k+1} + \varepsilon p^{k+1} - \varepsilon p^k) \end{aligned} \quad (\text{A.3})$$

and R_k is the part of $R(\mathbf{u}^{k+1}, p^{k+1})$ that depends only on \mathbf{u}^k and p^k :

$$R_k := -\mathbf{u}^k - (1 - \theta) \Delta t \nabla \cdot (2Re^{-1} \nabla^s \mathbf{u}^k) + (1 - \theta) \Delta t (\mathbf{u}^k \cdot \nabla) \mathbf{u}^k + (1 - \theta) \Delta t \nabla p^k.$$

The Newton iteration (\mathbf{u}^n, p^n) will yield an approximation to $(\mathbf{u}^{k+1}, p^{k+1})$, where n is the Newton iteration number. Thus, we need to solve

$$R(\mathbf{u}^n, p^n) = \mathbf{0}.$$

Newton's method reads

$$R'(\mathbf{u}^n, p^n)(\mathbf{u}^{n+1} - \mathbf{u}^n, p^{n+1} - p^n) = -R(\mathbf{u}^n, p^n),$$

where

$$[R'(\mathbf{u}^n, p^n)]_{ij} := \frac{\partial R_i(\mathbf{u}^n, p^n)}{\partial (\mathbf{u}^n, p^n)_j}$$

is the Jacobian of R . We explicitly construct the approximation to R' , element by element, from a sequence of finite differences

$$[R'(\mathbf{u}^n, \mathbf{p}^n)]_{ij} \approx \frac{R_i((\mathbf{u}^n, \mathbf{p}^n) + h\mathbf{e}_j) - R_i((\mathbf{u}^n, \mathbf{p}^n))}{h},$$

where h is the differencing parameter and \mathbf{e}_j is the j -th unit vector. The reason for using an explicit construction of the approximation to the Jacobian instead of using matrix-free Jacobian vector products is that we will need the actual Jacobian matrix in sensitivity computations in our longer-term research. We also note that our finite difference implementation for the Jacobian is ripe for automatic differentiation.

A.5. Computational Implementation. ViTLES is written on top of PETSc (the portable, extensible toolkit for scientific computing) developed at Argonne National Laboratory [4, 3, 5]. ViTLES makes use of MPI, linpack and the blas. We have also used ADIC, the automatic differentiation tool [26], to compute Jacobians. This allows us to rapidly and efficiently implement several problems of interest in CFD, e.g. closure modeling and sensitivity analysis. Routines have been developed to convert ViTLES format to several visualization routines including Tecplot, VTK and VU.

REFERENCES

- [1] R.A. Adams, *Sobolev spaces*, Academic Press, New York, 1975.
- [2] J.C. André, G.D. Moor, P. Lacarrere, and R.D. Vachat, *Turbulence approximations for inhomogeneous flows. Part i: The clipping approximation*, J. Atmos. Sci. **33** (1976), 476–481.
- [3] S. Balay, K. Buschelman, V. Eijkhout, W. D. Gropp, D. Kaushik, M. G. Knepley, L. Curfman McInnes, B. F. Smith, and H. Zhang, *PETSc users manual*, Tech. Report ANL-95/11 - Revision 2.1.5, Argonne National Laboratory, 2004.
- [4] S. Balay, K. Buschelman, W. D. Gropp, D. Kaushik, M. G. Knepley, L. Curfman McInnes, B. F. Smith, and H. Zhang, *PETSc Web page*, 2001, <http://www.mcs.anl.gov/petsc>.
- [5] S. Balay, V. Eijkhout, W. D. Gropp, L. Curfman McInnes, and B. F. Smith, *Efficient management of parallelism in object oriented numerical software libraries*, Modern Software Tools in Scientific Computing (E. Arge, A. M. Bruaset, and H. P. Langtangen, eds.), Birkhäuser Press, 1997, pp. 163–202.
- [6] L.C. Berselli, T. Iliescu, and W.J. Layton, *Mathematics of large eddy simulation of turbulent flows*, Springer Verlag, 2005.
- [7] J. Boussinesq, *Essai sur la théorie des eaux courantes.*, Mém. prés par div. savants à la Acad. Sci. **23** (1877), 1–680.
- [8] S. C. Brenner and L. R. Scott, *The mathematical theory of finite element methods*, Texts in Applied Mathematics, vol. 15, Springer-Verlag, New York, 1994. MR MR1278258 (95f:65001)
- [9] A. J. Chorin, *Numerical solution of the Navier-Stokes equations*, Math. Comp. **22** (1968), 745–762. MR MR0242392 (39 #3723)
- [10] G.-H. Cottet, *Artificial viscosity models for vortex and particle methods*, J. Comput. Phys. **127** (1996), 299–308.
- [11] G.-H. Cottet and A.A. Wray, *Anisotropic grid-based formulas for subgrid-scale models*, Annual Research Briefs, Center for Turbulence Research, Stanford University and NASA Ames, 1997, pp. 113–122.
- [12] M. Crouzeix and V. Thomée, *The stability in L_p and W_p^1 of the L_2 -projection onto finite element function spaces*, Math. Comp. **48** (1987), no. 178, 521–532. MR MR878688 (88f:41016)
- [13] C. Cuvelier, A. Segal, and A. A. van Steenhoven, *Finite element methods and Navier-Stokes equations*, Mathematics and its Applications, vol. 22, D. Reidel Publishing Co., Dordrecht, 1986. MR MR850259 (88g:65106)
- [14] A. Dörnbrack, *Turbulent mixing by breaking gravity waves*, J. Fluid Mech. **375** (1998), 113–141.
- [15] Q. Du and M. D. Gunzburger, *Finite-element approximations of a Ladyzhenskaya model for stationary incompressible viscous flow*, SIAM J. Numer. Anal. **27** (1990), no. 1, 1–19. MR MR1034917 (91e:65123)
- [16] ———, *Analysis of a Ladyzhenskaya model for incompressible viscous flow*, J. Math. Anal. Appl. **155** (1991), no. 1, 21–45. MR MR1089323 (92e:35134)

- [17] A. Ern and J.-L. Guermond, *Theory and practice of finite elements*, Applied Mathematical Sciences, vol. 159, Springer-Verlag, New York, 2004. MR MR2050138 (2005d:65002)
- [18] H. J. S. Fernando, *Aspects of stratified turbulence*, Developments in Geophysical Turbulence (R. M. Kerr and Y. Kimura, eds.), Kluwer, 2000, pp. 81–92.
- [19] U. Frisch, *Turbulence, the Legacy of A.N. Kolmogorov*, Cambridge University Press, Cambridge, 1995.
- [20] G. P. Galdi, *An introduction to the mathematical theory of the Navier-Stokes equations. Vol. I*, Springer Tracts in Natural Philosophy, vol. 38, Springer-Verlag, New York, 1994, Linearized steady problems. MR MR1284205 (95i:35216a)
- [21] G. P. Galdi, J. G. Heywood, and R. Rannacher (eds.), *Fundamental directions in mathematical fluid mechanics*, Advances in Mathematical Fluid Mechanics, Birkhäuser Verlag, Basel, 2000. MR MR1798752 (2001f:76004)
- [22] M. Germano, U. Piomelli, P. Moin, and W.H. Cabot, *A dynamic subgrid-scale eddy viscosity model*, Phys. Fluids A **3** (1991), 1760–1765.
- [23] S. Ghosal, T. S. Lund, P. Moin, and K. Akselvoll, *A dynamic localization model for large-eddy simulation of turbulent flows*, J. Fluid Mech. **286** (1995), 229–255. MR MR1336046 (96e:76070a)
- [24] V. Girault and P.-A. Raviart, *Finite element methods for Navier-Stokes equations*, Springer Series in Computational Mathematics, vol. 5, Springer-Verlag, Berlin, 1986, Theory and algorithms. MR MR851383 (88b:65129)
- [25] M. D. Gunzburger, *Finite element methods for viscous incompressible flows*, Computer Science and Scientific Computing, Academic Press Inc., Boston, MA, 1989, A guide to theory, practice, and algorithms. MR MR1017032 (91d:76053)
- [26] P. Hovland, B. Norris, and C. Bischof, *ADIC Web page*, 2005, <http://www-fp.mcs.anl.gov/adic/>.
- [27] T. Iliescu, *Genuinely nonlinear models for convection-dominated problems*, Comput. Math. Appl. **48** (2004), no. 10-11, 1677–1692. MR MR2107123 (2005h:76064)
- [28] T. Iliescu and P.F. Fischer, *Large Eddy Simulation of turbulent channel flows by the Rational LES model*, Phys. Fluids **15** (2003), no. 10, 3036–3047.
- [29] ———, *Backscatter in the Rational LES model*, Comput. & Fluids **35** (2004), no. 5-6, 783–790.
- [30] V. John, *Large eddy simulation of turbulent incompressible flows*, Lecture Notes in Computational Science and Engineering, vol. 34, Springer-Verlag, Berlin, 2004, Analytical and numerical results for a class of LES models. MR 2 018 955
- [31] V. John and W. J. Layton, *Analysis of numerical errors in large eddy simulation*, SIAM J. Numer. Anal. **40** (2002), no. 3, 995–1020 (electronic). MR MR1949402 (2004i:76132)
- [32] N. V. Kornev, I. V. Tkatchenko, and E. Hassel, *A simple clipping procedure for the dynamic mixed model based on Taylor series approximation*, Comm. Numer. Methods Engrg. **22** (2006), no. 1, 55–61.
- [33] O. A. Ladyžhenskaya, *New equations for the description of motion of viscous incompressible fluids and solvability in the large of boundary value problems for them*, Proc. Steklov Inst. Math. **102** (1967), 95–118.
- [34] O. A. Ladyžhenskaya, *Modifications of the Navier-Stokes equations for large gradients of the velocities*, Zap. Naučn. Sem. Leningrad. Otdel. Mat. Inst. Steklov. (LOMI) **7** (1968), 126–154. MR 39 #3169
- [35] W. J. Layton, *A nonlinear, subgrid-scale model for incompressible viscous flow problems*, SIAM J. Sci. Comput. **17** (1996), no. 2, 347–357. MR MR1374284 (96k:76073)
- [36] J. Leray and J. Schauder, *Topologie et équations fonctionnelles*, Ann. Sci. École Norm. Sup. (3) **51** (1934), 45–78. MR MR1509338
- [37] D.K. Lilly, *The representation of small scale turbulence in numerical simulation experiments*, Proc. IBM Sci. Computing Symp. On Environmental Sciences (Yorktown Heights, NY) (H.H. Goldstine, ed.), 1967, pp. 195–210.
- [38] P. J. Mason, *Large-eddy simulation of the convective atmospheric boundary layer*, J. Atmos. Sci. **46** (1989), 1492–1516.
- [39] C. Meneveau, T. Lund, and W. Cabot, *A Lagrangian dynamic subgrid-scale model of turbulence*, J. Fluid Mech. **319** (1996), 353–385.
- [40] J. W. Miles, *On the stability of heterogeneous shear flows*, J. Fluid Mech. **10** (1961), 496–508.
- [41] U. Piomelli, W.H. Cabot, P. Moin, and S. Lee, *Subgrid-scale backscatter in turbulent and transitional flow*, Phys. Fluids **3** (1991), no. 7, 1766–1771.
- [42] S.B. Pope, *Turbulent flows*, Cambridge University Press, Cambridge, 2000. MR 2003f:76002
- [43] F. Porté-Agel, C. Meneveau, and M. B. Parlange, *A scale-dependent dynamic model for large-eddy simulation: application to a neutral atmospheric boundary layer*, J. Fluid Mech. **415** (2000), 261–284. MR MR1775927 (2001e:76074)

- [44] A. Quarteroni and A. Valli, *Numerical approximation of partial differential equations*, Springer Series in Computational Mathematics, vol. 23, Springer-Verlag, Berlin, 1994. MR MR1299729 (95i:65005)
- [45] L.F. Richardson, *Weather prediction by numerical process*, Cambridge University Press, Cambridge, 1922.
- [46] J. J. Rohr, E. C. Itsweire, K. N. Helland, and C. W. Van Atta, *Growth and decay of turbulence in stably stratified shear flow*, J. Fluid Mech. **195** (1988), 77–111.
- [47] P. Sagaut, *Large eddy simulation for incompressible flows*, third ed., Scientific Computation, Springer-Verlag, Berlin, 2006, An introduction, Translated from the 1998 French original, With forewords by Marcel Lesieur and Massimo Germano, With a foreword by Charles Meneveau. MR MR2174208
- [48] U. Schumann, *Subgrid scale model for finite difference simulations of turbulent flows in plane channels and annuli*, J. Comput. Phys. **18** (1975), 376–404.
- [49] J.S. Smagorinsky, *General circulation experiments with the primitive equations*, Mon. Weather Review **91** (1963), 99–164.
- [50] B. Stevens, C.-H. Moeng, and P. P. Sullivan, *Large-eddy simulations of radiatively driven convection: Sensitivities to the representation of small scales*, J. Atmospheric Sci. **56** (1999), no. 23, 3963–3984.
- [51] D. Tafti, *Comparison of some upwind-biased high-order formulations with a second-order central-difference scheme for time integration of the incompressible Navier-Stokes equations*, Comput. & Fluids **25** (1996), no. 7, 647–665. MR MR1416431 (97i:65156)
- [52] E.R. van Driest, *On turbulent flow near a wall*, J. Aerospace Sci. **23** (1956), 1007–1011.
- [53] J. von Neumann and R.D. Richtmyer, *A method for the numerical calculation of hydrodynamic shocks*, J. Appl. Phys. **21** (1950), 232–237.
- [54] Y. Zang, R.L. Street, and J.R. Koseff, *A dynamic mixed subgrid-scale model and its application to turbulent recirculating flows*, Phys. Fluids A **5** (1993), no. 12, 3186–3196.